Journal of Physics: Conference Series **84** (2007) 012018 doi:10.1088/1742-6596/84/1/012018

Quantum measurements without Schrödinger cat states

D Spehner[1] **and F Haake**[2]

[1] Institut Fourier, 100 rue des Maths, 38402 Saint-Martin d'Hères, France
[2] Fachbereich Physik, Universität Duisburg-Essen, Lotharstrasse 1, 47048 Duisburg

E-mail: spehner@ujf-grenoble.fr

Abstract. We report and give an alternative derivation of some results on a model for a quantum measurement studied in [1]. The measured microscopic system is coupled to the position of a macroscopic pointer, which itself interacts with its environment via its momentum. The entanglement between the system and the pointer produced by their mutual interaction is simultaneous with the decoherence of distinct pointer readings resulting from leakage of information to the environment. After a discussion on the various time scales in the model we calculate the matrix elements of the system-pointer density operator between eigenstates of the measured observable with distinct eigenvalues. In general, the decay with time of these coherences is neither exponential nor gaussian. We determine the decoherence (decay) time in terms of the strength of the system-pointer and pointer-environment couplings. This decoherence time does not depend upon the details of the pointer-bath coupling as soon as it is smaller than the bath correlation time (non-Markov regime). In contrast, in the Markov regime it depends strongly on whether this coupling is Ohmic or super-Ohmic.

1. Introduction

The issue of the interpretation and theoretical description of measurements on quantum systems has been the subject of intense debates since the birth of quantum mechanics [2]. In the last three decades the major role played by environment-induced decoherence in measurement processes has been fully acknowledged thanks to the works of Zeh, Zurek and others (see [3, 4] and references therein). Various concrete models of a quantum system interacting with a measurement apparatus coupled to its environment have been investigated; some of them are inspired from statistical physics [5]. A renewal of interest for quantum detection and decoherence came in the last decade with new developments in quantum information. It is desirable to understand better the relation between quantum and classical information and how one can convert one into another. Moreover, a good control over all sources of decoherence is required to proceed quantum information. On the experimental side, measurements can be used both to extract information on quantum states and to monitor quantum systems (quantum trajectories [6], Zeno effect [7]). Experimental data are now available for the decoherence time in microwave cavities [8] and in solid state devices like superconducting tunnel junction nanocircuits [9,10].

A measurement on a quantum system consists in letting this system (called "object" in the following) interact with a measurement apparatus in such a way that some information about the object's state is transfered to the apparatus. It has been already recognised by Bohr (see e.g. [2]) that even though the composite (object and apparatus) system has to be described by the quantum theory, some part of the apparatus (called the "pointer" in the following) must be capable of a classical behaviour. In an ideal measurement, the interaction builds up a one-to-one correspondence between the eigenvalues s of the measured observable S (supposed here to have a discrete and non-degenerate spectrum) and some macroscopically distinguishable pointer states. These states may for instance

correspond to macroscopically distinct positions of the pointer. As is well-known [2–4] a quantum measurement involves both the establishment of the aforementioned object-apparatus correlations and some "superselection rules" destroying coherences between the pointer states. In most previous discussions in the literature these two processes are treated separately. A first step consists in establishing quantum correlations between the object and the pointer by means of an appropriate unitary evolution. This evolution results from an interaction and produces an object-pointer entangled state. If the object is initially in a superposition of eigenstates $|s\rangle$ of S, the unitary evolution builds up a Schrödinger cat state. This state is a superposition of separable object-pointer states given by tensor products of the eigenstates $|s\rangle$ with some pointer states having, say, sharply-defined positions depending on s. Macroscopic distances separate pointer locations corresponding to distinct s's. This Schrödinger cat state is taken as the initial state for a second dynamical process called decoherence, which leads to superselection rules. During this second step the quantum correlations between the object and apparatus are transformed into classical correlations, i.e., the superposition of the object-pointer product states is transformed into a statistical mixture of the same states.

For such a sequential treatment to make physical sense, the time duration of the entanglement process must be short compared with the decoherence time after which coherences in the superposition disappear. However, it is known that the latter time is extremely short. The sequential treatment of the entanglement and decoherence can then be difficult to achieve in practice. The purpose of this paper is to study a model in which the two above steps are performed simultaneously. If, in contrast to the situation described above, the decoherence time is the shorter time, macroscopically distinguishable superpositions are transformed into statistical mixtures faster than entanglement can create them. The whole measurement is then performed without producing a Schrödinger cat state as an intermediate step.

Our model is a three-partite system consisting in the microscopic object to be measured, a pointer composed by a single degree of freedom of the macroscopic apparatus, singled out by its strong coupling to the object, and a bath consisting of all other degrees of freedom of the apparatus. A pointer-bath coupling is responsible for decoherence. In an ideal measurement, the measured observable S in the Heisenberg picture is weakly changed during the measurement. This can be the case provided that, on the one hand, the object-pointer interaction Hamiltonian producing the aforementioned entanglement nearly commutes with S and, on the other hand, the time scale for significant evolution of S under the object Hamiltonian is much larger than the time duration of the measurement. In particular, this time scale must be large compared with the decoherence time $t_{\rm dec}$. Furthermore, $t_{\rm dec}$ is also much smaller than the classical time scale characterising the changes in position of the pointer under its proper Hamiltonian. As already acknowledged in [11] in the case of a system-bath coupling, explicit formulas for $t_{\rm dec}$ can be derived on the basis of this separation of time scales, with no further assumptions about the relation between $t_{\rm dec}$ and the bath correlation time T_B. This allows us to treat the pointer-bath coupling in a non-Markov regime $t_{\rm dec} \lesssim T_B$ as well as in the Markov regime $t_{\rm dec} \gg T_B$. Moreover, we need not to assume that the bath is composed of harmonic oscillators linearly coupled to the pointer, a supposition often made in previous studies. A third noteworthy generalisation with respect to previous works concerns the object-apparatus initial state. While it is appropriate to assume that the object and apparatus are uncorrelated initially, we shall consider two types of initial states for the apparatus in which the pointer and bath are either uncorrelated (i.e., in a product state) or in thermal equilibrium (i.e., in an entangled state) with each other.

The paper is organised as follows. The model is introduced in Section 2. We discuss the separation of the time scales and a subsequent simplification of the object-pointer dynamics in Section 3. Sections 4 and 5 contain a separate study of the two dynamical processes producing the entanglement of the object with the pointer and the loss of coherences between well-separated pointer readings. Section 6 provides a short summary of these two sections. We derive and discuss our results for a separable pointer-bath initial state in Section 7. In the next Section, we report without proofs the results derived in [1] for a pointer and bath initially entangled and in thermal equilibrium. Our conclusions are drawn in Section 9. Appendix A contains technical proofs of some statements made in Section 7.

2. The model

As in much of the previous literature on quantum measurement [3–5], we shall deal with a three-partite system: the object of measurement is some microscopic system ($\mathcal{S}$); a single-degree-of-freedom macroscopic pointer ($\mathcal{P}$) will allow read-outs; finally, a bath ($\mathcal{B}$) with many ($N \gg 1$) degrees of freedom serves to decohere distinct pointer readings. We shall have to deal with the following dynamical variables: for the object $\mathcal{S}$, the observable S to be measured; for $\mathcal{P}$ the position X and the momentum P; and for $\mathcal{B}$, a certain coupling agent B. The pointer is coupled to $\mathcal{S}$ and $\mathcal{B}$ via the Hamiltonians

$$H_{\mathcal{PS}} = \epsilon SP \quad , \quad H_{\mathcal{PB}} = BX^{\alpha} \tag{1}$$

where ϵ is a coupling constant and α a positive integer. The object-pointer coupling $H_{\mathcal{PS}}$ is chosen so as to (i) not change the object observable S to be measured (i.e., $[H_{\mathcal{PS}}, S] = 0$); (ii) be capable of shifting the pointer position by an amount proportional to (the eigenvalues of) S, in such a way that each eigenvalue s of S becomes *entangled* with a specific pointer reading; (iii) be a strong coupling (ϵ is large), so that different eigenvalues $s \neq s'$ eventually become associated with pointer readings separated by large distances. The pointer-bath interaction, in turn, is chosen for most efficient *decoherence* of distinct pointer positions [11]. Depending on the value of α, nonlinear ($\alpha > 1$) as well as linear ($\alpha = 1$) couplings will be considered. The free evolutions of $\mathcal{S}$, $\mathcal{P}$ and $\mathcal{B}$ are generated by respective Hamiltonians $H_{\mathcal{S}}$, $H_{\mathcal{P}}$ and $H_{\mathcal{B}}$. We do not have to specify $H_{\mathcal{S}}$ explicitly. The pointer Hamiltonian $H_{\mathcal{P}} = P^2/2M + V(X)$ has a potential $V(x)$ with a local minimum at $x = 0$, so that $V'(0) = 0$ and $V''(0) > 0$; moreover, the potential barriers at the left and right of this minimum have a height V_0 satisfying $V_0 \gg k_B T$, where T is the temperature and k_B the Boltzmann constant. An example of such potential is sketched in Fig. 1. A confining potential with a single minimum at $x = 0$ provides another example, for which $V_0 = \infty$. The Hamiltonian of the full system $\mathcal{S} + \mathcal{P} + \mathcal{B}$ is

$$H = H_{\mathcal{S}} + H_{\mathcal{P}} + H_{\mathcal{B}} + H_{\mathcal{PS}} + H_{\mathcal{PB}} \, . \tag{2}$$

We now proceed to describe the initial states of the object $\mathcal{S}$ and the apparatus $\mathcal{P} + \mathcal{B}$ allowed for. It is appropriate to require initial statistical independence between $\mathcal{S}$ and $\mathcal{P} + \mathcal{B}$. The initial density operator $\rho_{\mathcal{S}}$ of the object may represent a pure or a mixed state. Two types of initial conditions for the apparatus will be considered. The first one, to be referred to as partial equilibrium, is a product state in which $\mathcal{P}$ has some density operator $\rho_{\mathcal{P}}$ and $\mathcal{B}$ is at thermal equilibrium with the Gibbs density operator $\rho_{\mathcal{B}}^{(\mathrm{eq})} = Z_{\mathcal{B}}^{-1} \exp(-\beta H_{\mathcal{B}})$, wherein $\beta = (k_B T)^{-1}$ is the inverse temperature. For this first initial state all three subsystems are statistically independent. In the second (more realistic) initial state, the apparatus $\mathcal{P} + \mathcal{B}$ is in thermal equilibrium according to the density operator $\rho_{\mathcal{PB}}^{(\mathrm{eq})} = Z_{\mathcal{PB}}^{-1} \, \mathrm{e}^{-\beta(H_{\mathcal{P}} + H_{\mathcal{B}} + H_{\mathcal{PB}})}$. For a pointer potential as sketched in Fig.1, this thermal equilibrium must be understood as a local equilibrium around $x = 0$. It can be achieved by first preparing $\mathcal{P}$ in some state localised near $x = 0$ at a time $t = -t_{\mathrm{in}}$, with t_{in} larger than the relaxation rate but small with respect to the tunnelling escape rate, and then letting $\mathcal{P}$ interact with $\mathcal{B}$ until $t = 0$. The two initial states of $\mathcal{S} + \mathcal{P} + \mathcal{B}$ are

$$\rho(0) = \rho_{\mathcal{S}} \otimes \rho_{\mathcal{P}} \otimes \rho_{\mathcal{B}}^{(\mathrm{eq})} \qquad \text{partial-equilibrium apparatus} \tag{3}$$

$$\rho(0) = \rho_{\mathcal{S}} \otimes \rho_{\mathcal{PB}}^{(\mathrm{eq})} \qquad \text{equilibrium apparatus} \, . \tag{4}$$

We further specify the partial-equilibrium state (3) by requiring that the probability density $\langle x|\rho_{\mathcal{P}}|x\rangle$ to find the pointer at position x has a single peak of width $\Delta x = \Delta$ centred at $x = 0$. A momentum uncertainty $\Delta p = 2\pi\hbar/\lambda$ defines a second length scale λ. A macroscopic pointer has both Δ and λ negligibly small against any macroscopic read-out scale Δ_{class},

$$\lambda \leq 4\pi\Delta \ll \Delta_{\mathrm{class}} \, , \tag{5}$$

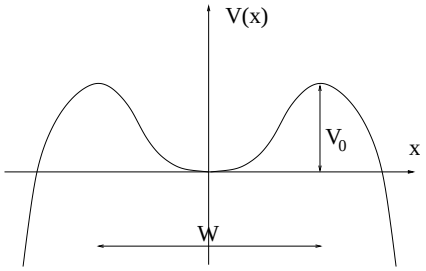

Figure 1. Sketch of a candidate for the pointer potential. The height V_0 of the potential barriers around $x = 0$ and the width of the potential wall, $W \approx (V_0/V''(0))^{1/2}$, are much larger than k_BT and the thermal fluctuation $\Delta_{\rm th} = (k_BT/V''(0))^{1/2}$. The unstable parts of $V(x)$ at the left and right of the barriers serves to amplify the separation between the peaks in the pointer density produced by its interaction with the object. Such an amplification can happen after the object-pointer coupling is turned off at a time $t_{\rm int} > W/(\epsilon\delta s)$ (see Section 6).

where the first inequality is the uncertainty principle. We shall also require that

$$\frac{\lambda\Delta}{2\pi\hbar} = \frac{\Delta}{\Delta p} \approx (MV''(0))^{-1/2} \tag{6}$$

which means that the state $\rho_{\mathcal{P}}$ is not highly squeezed in momentum nor in position. As a concrete example we may consider a Gaussian pointer density matrix,

$$\langle x|\rho_{\mathcal{P}}|x'\rangle = \frac{1}{\sqrt{2\pi\Delta^2}}\,{\rm e}^{-(x+x')^2/(8\Delta^2)}\,{\rm e}^{-2\pi^2(x-x')^2/\lambda^2}\ . \tag{7}$$

If $\mathcal{P}$ is initially in a pure state then ${\rm tr}_{\mathcal{P}}\,\rho_{\mathcal{P}}^2 = \int {\rm d}x\,{\rm d}x'\langle x|\rho_{\mathcal{P}}|x'\rangle^2 = 1$, which implies that this state has the minimum uncertainty product $\Delta x\Delta p = \hbar/2$, i.e., $\lambda = 4\pi\Delta$. The Gaussian density (7) also arises if $\mathcal{P}$ is in a Gibbs state $\rho_{\mathcal{P}}^{(\rm eq)} = Z_{\mathcal{P}}^{-1}{\rm e}^{-\beta H_{\mathcal{P}}}$ at high enough temperature. To see this, we note that the pointer observables X and P evolve noticeably under the Hamiltonian $H_{\mathcal{P}}$ on a *classical time scale* $T_{\mathcal{P}}$, which is much larger than all other (quantum) time scales in the model. In particular, $T_{\mathcal{P}}$ is much larger than the thermal time, $T_{\mathcal{P}} \gg \hbar\beta$. As a result, the matrix elements $\langle x|\rho_{\mathcal{P}}^{(\rm eq)}|x'\rangle$ of $\rho_{\mathcal{P}}^{(\rm eq)}$ can be approximated by $Z_{\mathcal{P}}^{-1}{\rm e}^{-\beta(V(x)+V(x'))/2}{\rm e}^{-2\pi^2(x-x')^2/\lambda_{\rm th}^2}$, wherein $\lambda_{\rm th} = 2\pi\hbar(\beta/M)^{1/2}$ is the thermal de Broglie wavelength. The reader may recognise in this expression the short-time behaviour of the quantum propagator $\langle x|{\rm e}^{-{\rm i}tH_{\mathcal{P}}/\hbar}|x'\rangle$ for $t = -{\rm i}\hbar\beta$ (see e.g. [12]). Since the potential $V(x)$ has a local minimum at $x = 0$, it can be approximated near the origin by a quadratic potential, $V(x) \simeq V(0) + x^2V''(0)/2$. Therefore, for small x and x' , $\langle x|\rho_{\mathcal{P}}^{(\rm eq)}|x'\rangle$ has the Gaussian form (7) with $\Delta = \Delta_{\rm th} = (\beta V''(0))^{-1/2}$ and $\lambda \simeq \lambda_{\rm th}$. It is important to bear in mind the separation of length scales $\lambda_{\rm th} \ll \Delta_{\rm th} \ll \Delta_{\rm class}$. Inasmuch as the pointer classical time scale $T_{\mathcal{P}}$ may be defined as $T_{\mathcal{P}} = (M/V''(0))^{1/2}$, the fact that $\lambda_{\rm th}$ is much smaller than $\Delta_{\rm th}$ is equivalent to $T_{\mathcal{P}} \gg \hbar\beta$. To fix ideas, for $T_{\mathcal{P}} = 1$ s, $M = 1$ g, $\Delta_{\rm class} = 1$ cm and a temperature of 1 K, the above-mentioned length scales differ by more than eight orders of magnitude. Hence (5) and (6) are well satisfied if $\rho_{\mathcal{P}} = \rho_{\mathcal{P}}^{(\rm eq)}$.

All of these illustrations, including the Gaussian (7), are meant to give an intuitive picture. What we shall need in actual fact are the quasi-classical nature of the pointer initial state, as implied by (5) and (6), together with the single-peak character of the initial density of pointer positions.

We will study in what follows the dynamics of the reduced state of $\mathcal{S} + \mathcal{P}$ (object and pointer). This state is defined by a density operator $\rho_{\mathcal{PS}}(t)$ obtained by tracing out the bath degrees of freedom in the state of $\mathcal{S} + \mathcal{P} + \mathcal{B}$,

$$\rho_{\mathcal{PS}}(t) = {\rm tr}_{\mathcal{B}}\left({\rm e}^{-{\rm i}tH/\hbar}\rho(0)\,{\rm e}^{{\rm i}tH/\hbar}\right)\ . \tag{8}$$

Here and in what follows ${\rm tr}_j$ refers to the partial trace over the Hilbert space of $j = \mathcal{S}, \mathcal{P}$ or $\mathcal{B}$.

3. Time scales

3.1. The time scales of the object, pointer and bath

Let us denote by $\widetilde{S}(t)$ the time-evolved observable S in the absence of the coupling $H_{\mathcal{PS}}$, i.e., for the dynamics implemented by the "free Hamiltonian" $H_{\mathcal{S}}$. Similarly, let $\widetilde{X}(t)$ and $\widetilde{B}(t)$ be the time-evolved observables X and B when both couplings $H_{\mathcal{PS}}$ and $H_{\mathcal{PB}}$ are turned off. Namely,

$$\widetilde{O}_j(t) = \mathrm{e}^{\mathrm{i}tH_j/\hbar} O_j \, e^{-\mathrm{i}tH_j/\hbar} \quad , \quad O = S, X \text{ or } B \quad , \quad j = \mathcal{S}, \mathcal{P} \text{ or } \mathcal{B} \, . \tag{9}$$

One may associate with the time evolution of $\widetilde{X}(t)$, $\widetilde{B}(t)$ and $\widetilde{S}(t)$ four distinct time scales. The time scale $T_{\mathcal{P}} = (M/V''(0))^{1/2}$ has been already introduced above; it is the time scale for significant evolution of $\widetilde{X}(t)$ (or, equivalently, of $\widetilde{P}(t) = M\mathrm{d}\widetilde{X}/\mathrm{d}t$) when the pointer is in the initial state $\rho_{\mathcal{P}}$. If $\rho_{\mathcal{P}}$ is a pure state, its energy uncertainty ΔE is given by Heisenberg's uncertainty relation $\Delta E \approx 2\pi\hbar/T_{\mathcal{P}}$. In fact, $\Delta E^2 = \mathrm{tr}_{\mathcal{P}}({H_{\mathcal{P}}}^2 \, \rho_{\mathcal{P}}) - \mathrm{tr}_{\mathcal{P}}(H_{\mathcal{P}} \, \rho_{\mathcal{P}})^2$ is found by means of (7) to be equal to $(2\pi\hbar)^4/(2\lambda^4 M^2) + V''(0)^2\Delta^4/2 - \hbar^2 V''(0)/(4M)$; one can check that the three terms in this expression are of the order of $\hbar^2/{T_{\mathcal{P}}}^2$ by combining $\lambda = 4\pi\Delta$ and (6).

The *bath correlation time* $T_{\mathcal{B}}$ is defined with the help of the bath auto-correlation function

$$h(t) = \mathrm{tr}_{\mathcal{B}} \left(\widetilde{B}(t) B \rho_{\mathcal{B}}^{(\mathrm{eq})} \right) \, . \tag{10}$$

For simplicity, it is assumed here and in the whole paper that

$$\mathrm{tr}_{\mathcal{B}}(B\rho_{\mathcal{B}}^{(\mathrm{eq})}) = 0 \, . \tag{11}$$

Because the bath has many degrees of freedom, $h(t)$ decays (often exponentially) to zero as $|t|$ goes to infinity. We define $T_{\mathcal{B}}$ (respectively $t_{\mathcal{B}}$) as the largest (smallest) time constant characterising the variations of h. More precisely, $h(t) \simeq 0$ whenever $|t| \gg T_{\mathcal{B}}$ and $h(t) \simeq h(0)$ whenever $|t| \ll t_{\mathcal{B}}$. Note that with $\mathcal{B}$ in thermal equilibrium, the thermal time $\hbar\beta$ figures among the decay rates of h and thus $t_{\mathcal{B}} \leq \hbar\beta \leq T_{\mathcal{B}}$.

The time scale $T_{\mathcal{S}}$ is defined in an analogous way as $t_{\mathcal{B}}$, so as to signal significant variation of the mean value $\mathrm{tr}_{\mathcal{S}}(\widetilde{S}(t)\rho_{\mathcal{S}})$ of $\widetilde{S}(t)$ and of the object correlation functions such as $\mathrm{tr}_{\mathcal{S}}(\widetilde{S}(t)S\rho_{\mathcal{S}})$. Let us stress that $T_{\mathcal{S}}$ can be larger than the inverse of the typical object Bohr frequency $(E - E')/\hbar$ (here E and E' denote two neighbouring eigenvalues of $H_{\mathcal{S}}$). For instance, if S is (or commutes with) the energy $H_{\mathcal{S}}$, then $T_{\mathcal{S}} = \infty$.

3.2. Separation of time scales

As stressed in the Introduction, during the time span of an ideal measurement the measured observable $\widetilde{S}(t)$ does not evolve noticeably under the "free" Hamiltonian $H_{\mathcal{S}}$. The same conclusion holds for the pointer observables $\widetilde{X}(t)$ and $\widetilde{P}(t)$, which evolve noticeably on the classical time scale $T_{\mathcal{P}}$. It is thus legitimate to assume that the object and pointer are put in contact during a time t_{int} *much shorter than both* $T_{\mathcal{S}}$ *and* $T_{\mathcal{P}}$. As far as we are aware, this natural separation of time scales in a quantum measurement has not been so far fully exploited in previous works. We will see below that it allows for a great simplification of the dynamics implemented by the Hamiltonian (2). The density matrix (8) can then be determined at time t_{int} without relying on an allegedly short bath correlation time $T_{\mathcal{B}} \ll t_{\mathrm{int}}$ (Markov approximation) and without making a specific choice for the pointer-bath interaction (among such choices, the quantum Brownian motion and the spin-boson model are widely discussed in the literature, see [4,18,19] and references therein). In fact, we will see in this Section that for $t_{\mathrm{int}} \ll T_{\mathcal{S}}, T_{\mathcal{P}}$ the Hamiltonians $H_{\mathcal{S}}$ and $H_{\mathcal{P}}$ can be dropped out in the total Hamiltonian (2) provided that the initial conditions (3) or (4) are modified appropriately.

For times $t \ll T_{\mathcal{S}}, T_{\mathcal{P}}$, the object-apparatus evolution operator can be approximated by

$$\mathrm{e}^{-\mathrm{i}tH/\hbar} \simeq \mathrm{e}^{-\mathrm{i}t(H_{\mathcal{S}}+H_{\mathcal{P}})/\hbar} \mathrm{e}^{-\mathrm{i}t(H_{\mathcal{B}}+H_{\mathcal{PS}}+H_{\mathcal{PB}})/\hbar} \quad , \quad |t| \ll T_{\mathcal{S}}, T_{\mathcal{P}} \, . \tag{12}$$

This can be established by expressing this evolution operator in the interaction picture with respect to $H_0 = H_{\mathcal{S}} + H_{\mathcal{P}}$. By (1) and (2),

$$\mathrm{e}^{\mathrm{i}tH_0/\hbar}\mathrm{e}^{-\mathrm{i}tH/\hbar} = \mathcal{T}\exp\left\{-\frac{\mathrm{i}}{\hbar}\int_0^t \mathrm{d}\tau\left(H_{\mathcal{B}} + \epsilon\,\widetilde{S}(\tau)\widetilde{P}(\tau) + B\widetilde{X}(\tau)^\alpha\right)\right\} \tag{13}$$

wherein $\mathcal{T}$ denotes the time-ordering and $\widetilde{S}(\tau)$, $\widetilde{P}(\tau)$ and $\widetilde{X}(\tau)$ are given by (9). Note that for $|t| \ll T_{\mathcal{S}}, T_{\mathcal{P}}$ these operators are almost constant in time between $\tau = 0$ and $\tau = t$. Hence one may replace them in (13) by S, P and X, respectively. In other words, the right-hand side of (13) can be approximated by $\exp\{-\mathrm{i}t(H_{\mathcal{B}} + H_{\mathcal{PS}} + H_{\mathcal{PB}})/\hbar\}$. Multiplying both members of (13) by $\mathrm{e}^{-\mathrm{i}tH_0/\hbar}$, one obtains (12).

Let us substitute t by $-t$ in (12), take the adjoint and replace the result into (8). One then finds that the impact of $H_{\mathcal{S}}$ and $H_{\mathcal{P}}$ on the dynamics of $\rho_{\mathcal{PS}}(t)$ can be fully accounted for at times $t \ll T_{\mathcal{S}}, T_{\mathcal{P}}$ by modifying the initial state of $\mathcal{S} + \mathcal{P} + \mathcal{B}$ according to

$$\rho(0) \longrightarrow \mathrm{e}^{-\mathrm{i}t(H_{\mathcal{S}}+H_{\mathcal{P}})/\hbar}\rho(0)\,\mathrm{e}^{\mathrm{i}t(H_{\mathcal{S}}+H_{\mathcal{P}})/\hbar}\,. \tag{14}$$

After this slippage of the initial condition, one makes a negligible error in (8) by dropping out $H_{\mathcal{S}}$ and $H_{\mathcal{P}}$ in the total Hamiltonian (2).

Thanks to the quasi-classical nature of the pointer initial state $\rho_{\mathcal{P}}$ in (3), this state is not modified by the substitution (14). This can be justified as follows if $\rho_{\mathcal{P}}$ is a pure state. Let $|E_k\rangle$ be the eigenvectors of $H_{\mathcal{P}}$ with eigenenergies E_k. We set $\rho_{\mathcal{P}}^{(0)}(t) = \mathrm{e}^{-\mathrm{i}tH_{\mathcal{P}}/\hbar}\rho_{\mathcal{P}}\,\mathrm{e}^{\mathrm{i}tH_{\mathcal{P}}/\hbar}$. Then

$$\langle E_k|\rho_{\mathcal{P}}^{(0)}(t)|E_l\rangle = \mathrm{e}^{-\mathrm{i}t(E_k-E_l)/\hbar}\langle E_k|\rho_{\mathcal{P}}|E_l\rangle \simeq \langle E_k|\rho_{\mathcal{P}}|E_l\rangle \quad , \quad t \ll T_{\mathcal{P}}\,. \tag{15}$$

Indeed, if $|E_k - E_l|$ is of the order of (or smaller than) the energy uncertainty $\Delta E \approx 2\pi\hbar/T_{\mathcal{P}}$ then the phase factor in the second member of (15) is close to unity when $t \ll T_{\mathcal{P}}$; otherwise $\langle E_k|\rho_{\mathcal{P}}|E_l\rangle \simeq 0$. One can also show [1] that $\rho_{\mathcal{P}}^{(0)}(t) \simeq \rho_{\mathcal{P}}$ at times $t \ll T_{\mathcal{P}}$ if $\rho_{\mathcal{P}}$ is a gaussian mixed state given by (7) and, for the initial condition (4), it holds $\mathrm{e}^{-\mathrm{i}tH_{\mathcal{P}}/\hbar}\rho_{\mathcal{PB}}^{(\mathrm{eq})}\,\mathrm{e}^{\mathrm{i}tH_{\mathcal{P}}/\hbar} \simeq \rho_{\mathcal{PB}}^{(\mathrm{eq})}$ provided that $t, \hbar\beta \ll T_{\mathcal{P}}$. The situation is different for the object initial state $\rho_{\mathcal{S}}$: then

$$\rho_{\mathcal{S}}^{(0)}(t) = \mathrm{e}^{-\mathrm{i}tH_{\mathcal{S}}/\hbar}\rho_{\mathcal{S}}\,\mathrm{e}^{\mathrm{i}tH_{\mathcal{S}}/\hbar} \tag{16}$$

cannot be approximated by $\rho_{\mathcal{S}}$. For instance, for $S = H_{\mathcal{S}}$ it has been argued above that $T_{\mathcal{S}} = \infty$ and $\langle s|\rho_{\mathcal{S}}^{(0)}(t)|s'\rangle = \mathrm{e}^{-\mathrm{i}t(s-s')/\hbar}\langle s|\rho_{\mathcal{S}}|s'\rangle$ is certainly not close to $\langle s|\rho_{\mathcal{S}}|s'\rangle$ for all finite times t, excepted for the diagonal matrix elements $\langle s|\rho_{\mathcal{S}}^{(0)}(t)|s\rangle = \langle s|\rho_{\mathcal{S}}|s\rangle$. For general observables S, these diagonal elements still almost coincide when $t \ll T_{\mathcal{S}}$. Actually, in view of the definition of $T_{\mathcal{S}}$ (Subsection 3.1), $\mathrm{tr}(\widetilde{S}(t)\rho_{\mathcal{S}}) = \sum_s s\langle s|\rho_{\mathcal{S}}^{(0)}(t)|s\rangle$ has to approximate $\mathrm{tr}(S\rho_{\mathcal{S}}) = \sum_s s\langle s|\rho_{\mathcal{S}}|s\rangle$ in this limit.

It follows from the above discussion that it is well justified to set $H = H_{\mathcal{B}} + H_{\mathcal{PS}} + H_{\mathcal{PB}}$ in (8) at times $t \ll T_{\mathcal{S}}, T_{\mathcal{P}}$ provided that $\rho_{\mathcal{S}}$ is replaced in the initial conditions (3) and (4) by the time-dependent density operator (16).

4. Entanglement of the object and pointer

Before studying the dynamics generated by the total Hamiltonian (2), it is instructive to discuss what happens if one disregards the free dynamics of $\mathcal{S}$, $\mathcal{P}$ and $\mathcal{B}$ as well as the pointer-bath interaction, so that $H = H_{\mathcal{PS}} = \epsilon SP$. In such a situation the bath can be ignored. The initial product state of $\mathcal{S}$ and $\mathcal{P}$ evolves into an *entangled state* in which each eigenstate $|s\rangle$ of S is tied up with a given pointer position depending on s. Recalling that P is the generator of space translations we have

$\mathrm{e}^{\mathrm{i}\epsilon SPt/\hbar}|s,x\rangle = |s,x-t\epsilon s\rangle$ where $|s,x\rangle$ is the joint eigenstate of S and X with eigenvalues s and x, normalised as $\langle s,x|s',x'\rangle = \delta_{ss'}\delta(x-x')$. Hence an initial product state of $\mathcal{S}+\mathcal{P}$ becomes at time t

$$\rho_{\mathcal{PS}}(t) = \mathrm{e}^{-\mathrm{i}tH_{\mathcal{PS}}/\hbar}\rho_{\mathcal{S}}\otimes\rho_{\mathcal{P}}\,\mathrm{e}^{\mathrm{i}tH_{\mathcal{PS}}/\hbar} = \sum_{s,s'}\langle s|\rho_{\mathcal{S}}|s'\rangle\ |s\rangle\langle s'|\otimes\rho_{\mathcal{P},s,s'}(t)\ , \tag{17}$$

$$\rho_{\mathcal{P},s,s'}(t) = \int \mathrm{d}x\,\mathrm{d}x'\,\langle x_s(t)|\rho_{\mathcal{P}}|x'_{s'}(t)\rangle|x\rangle\langle x'| \quad , \quad x_s(t) = x - t\epsilon s\,, \quad x'_{s'}(t) = x' - t\epsilon s'\ . \tag{18}$$

It is now well to put forth a specification: Throughout the present paper we assume for simplicity that S *has a discrete and non-degenerate spectrum*. Moreover, if the Hilbert space of $\mathcal{S}$ has infinite dimension we restrict ourselves to initial states of the object satisfying $\langle s|\rho_{\mathcal{S}}|s'\rangle = 0$ if s or s' belong to a part of the spectrum containing arbitrarily close eigenvalues (near an accumulation point).

In the state (17), the diagonal object operator $\langle s|\rho_{\mathcal{S}}|s\rangle|s\rangle\langle s|$ is multiplied by the initial pointer density matrix $\rho_{\mathcal{P}}$ shifted by $t\epsilon s$ in position space, as given by (18) with $s'=s$. The interaction has thus tied up each eigenstate $|s\rangle$ of S with a pointer state which have position $x \simeq t\epsilon s$ with uncertainty Δ and momentum $p \simeq 0$ with uncertainty $2\pi\hbar/\lambda$. The probability density to find $\mathcal{P}$ at position x given that $\mathcal{S}$ is in the state $|s\rangle\langle s|$ has a single peak at $x = \epsilon st$ with a width Δ. The peaks corresponding to different values of s are separated by at least the distance $t\epsilon\delta s$, where δs is the minimum of $|s-s'|$ over all pairs (s,s') of non-degenerate eigenvalues such that $\langle s|\rho_{\mathcal{S}}|s'\rangle \neq 0$. In order to be able to infer the value of s from the position of the pointer, one must wait until all peaks are well resolved. That resolvability begins at the *entanglement time*

$$t_{\mathrm{ent}} = \frac{\Delta}{\epsilon\,\delta s}\ . \tag{19}$$

At that time, the reduced pointer density operator $\rho_{\mathcal{P}}(t) = \mathrm{tr}_{\mathcal{S}}(\rho_{\mathcal{PS}}(t))$ has a Wigner function represented in Fig.2. Much later yet, the separation between the peaks reaches a macroscopic value Δ_{class} at the time

$$t_{\mathrm{class}} = \frac{\Delta_{\mathrm{class}}}{\epsilon\,\delta s} \gg t_{\mathrm{ent}}\ , \tag{20}$$

allowing for a "reading" of the result by a classical observer.

The entanglement in $\rho_{\mathcal{PS}}(t)$ comes from the presence of the off-diagonal object operators $\langle s|\rho_{\mathcal{S}}|s'\rangle|s\rangle\langle s'|$ in (17). These operators are multiplied by the (non self-adjoint) pointer operators (18), the matrix elements of which have a peak at $(x,x') = (\epsilon st, \epsilon s't)$ with a height $(2\pi\Delta^2)^{-1/2}$ and a width dominated by Δ in both x and x'-directions of the (x,x')-plane. Therefore, the modulus of the matrix elements $\langle s,x|\rho_{\mathcal{PS}}(t)|s',x'\rangle$ for fixed $s\neq s'$ reaches its maximal value when $x=\epsilon st$ and $x'=\epsilon st$. For those values of x and x',

$$\langle s, x=\epsilon ts|\rho_{\mathcal{PS}}(t)|s', x'=\epsilon ts'\rangle = \langle s|\rho_{\mathcal{S}}|s'\rangle\,\langle 0|\rho_{\mathcal{P}}|0\rangle \tag{21}$$

is time-independent and proportional to $\langle s|\rho_{\mathcal{S}}|s'\rangle$. Hence all coherences between different eigenstates of S present in the initial state of the object are still alive, no matter how large the time t is. At times $t \gtrsim t_{\mathrm{class}}$, $\rho_{\mathcal{PS}}(t)$ resembles a Schrödinger cat state, i.e., has nonzero matrix elements between macroscopically distinguishable pointer position eigenstates. For such an object-pointer state, no classical probabilistic interpretation is possible: one cannot assign a probability to the pointer being located e.g. in the vicinity of $x=\epsilon ts$, henceforth implying that S has the value s. In a quantum measurement, the entanglement process must be completed by a decoherence process suppressing the coherences (21). We describe such a decoherence process in the next Section.

5. Decoherence and disentanglement of the object and pointer

Let us now turn to the dynamics generated by $H = H_{\mathcal{PB}}$ only, momentarily disregarding all other terms in the Hamiltonian (2). The coupling between $\mathcal{P}$ and $\mathcal{B}$ allows for decoherence: As shown in [11] for

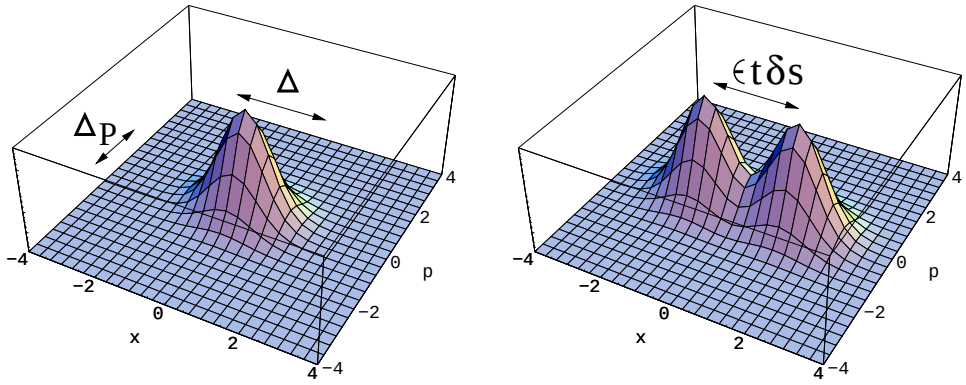

Figure 2. Wigner function of the pointer reduced state $\rho_{\mathcal{P}}(t)$ at time $t = 0$ (left) and $t \approx t_{\rm ent}$ (right) if the observable S is a spin one-half with two eigenvalues $\pm\delta s/2$.

a similar model, a quantum superposition of coherent states of $\mathcal{P}$ with well-separated peaks in position evolves under $H_{\mathcal{PB}}$ to a statistical mixture of these coherent states. If $\mathcal{S}$ and $\mathcal{P}$ are entangled, this also modifies the state of $\mathcal{S}$. We recall in this Section the fundamental role played by decoherence in quantum measurements (for more details, see [3–5]).

Assume object and pointer at time t_0 entangled, with $\rho_{\mathcal{PS}} = \rho^{\rm ent}_{\mathcal{PS}}$ given by (17); the time t_0 should be chosen larger than $t_{\rm ent}$, possibly as large as the classical time scale introduced above, $t_{\rm ent} \ll t_0 \approx t_{\rm class}$. At time t_0, the state of $\mathcal{S}+\mathcal{P}+\mathcal{B}$ is $\rho(t_0) = \rho^{\rm ent}_{\mathcal{PS}} \otimes \rho_{\mathcal{B}}$ and the pointer-bath coupling $H_{\mathcal{PB}}$ is switched on. The object-pointer matrix elements $\langle s, x|\rho^{\rm ent}_{\mathcal{PS}}|s', x'\rangle$ almost vanish for all (x, x') excepted for $x \simeq t_0\epsilon s$ and $x' \simeq t_0\epsilon s'$ with uncertainty Δ. At time $t > t_0$, the object-pointer density operator is defined by (8) with $H = H_{\mathcal{PB}}$. One can show [11] that for a coupling Hamiltonian of the form (1) the coherences $\langle s, x|\rho_{\mathcal{PS}}(t)|s', x'\rangle$ decay with the time span $t-t_0$ like gaussian if $x \neq x'$. The corresponding decay rates are given by $t_{\rm dec}(x, x')^{-1} = |x'^{\alpha} - x^{\alpha}|\sqrt{\langle B^2\rangle}/(\sqrt{2}\,\hbar)$. If $s \neq s'$, $x \simeq t_0\epsilon s$, $x' \simeq t_0\epsilon s'$ and $t_0 \simeq t_{\rm class}$, this decay brought about by the pointer-bath coupling requires a time span $t_{\rm dec}(x, x') \simeq t_{\rm dec}(t_0\epsilon s, t_0\epsilon s')$ much smaller than the dissipation time scale on which the pointer-bath coupling can irreversibly change the pointer position. Let us define the decoherence time $t_{\rm dec}$ as the largest of the times $t_{\rm dec}(t_0\epsilon s, t_0\epsilon s')$ for all distinct eigenvalues s, s' such that $\langle s|\rho_{\mathcal{S}}|s'\rangle \neq 0$. For $t - t_0 \gg t_{\rm dec}$, the object-pointer state has shed all terms $s \neq s'$ in the double sum in the density operator (17),

$$\rho_{\mathcal{PS}}(t) \simeq \sum_s \langle s|\rho_{\mathcal{S}}|s\rangle\, |s\rangle\langle s| \otimes \rho^{(s)}_{\mathcal{P}}(t)\ , \tag{22}$$

$$\rho^{(s)}_{\mathcal{P}}(t) = \int {\rm d}x\, {\rm d}x'\, \langle x_s(t_0)|\rho_{\mathcal{P}}|x'_s(t_0)\rangle\, {\rm e}^{-(t-t_0)^2/t_{\rm dec}(x,x')^2} |x\rangle\langle x'|\ , \tag{23}$$

wherein it has been assumed that $t_{\rm dec} \ll t - t_0 \ll t_{\mathcal{B}}, T_{\mathcal{S}}, T_{\mathcal{P}}$ (so that $H_{\mathcal{B}}$, $H_{\mathcal{S}}$ and $H_{\mathcal{P}}$ can be neglected) and $t_{\rm ent} \ll t_0 \approx t_{\rm class}$. While $\rho_{\mathcal{PS}}(t)$ is not (and actually never can become) strictly diagonal in the position basis of the pointer, the matrix elements of the pointer state (23) almost vanish if $|x - x'|$ is larger than either the uncertainty λ (see (7)) or the decoherence length $\sqrt{2}\hbar/(\alpha\,\Delta^{\alpha-1}(t - t_0)\sqrt{\langle B^2\rangle})$ (see the second factor inside the integral in (23)).

It is worth noting that the object-pointer states appearing in the sum over s in (22) are product states; $\rho_{\mathcal{PS}}(t)$ is a statistical mixture of these states with probabilities $p_s = \langle s|\rho_{\mathcal{S}}|s\rangle$. Hence the decoherence *disentangles* $\mathcal{S}$ and $\mathcal{P}$. This implies that in the time regime indicated after (23), $\mathcal{S}$ and $\mathcal{P}$ can be given independent states $\rho_{\mathcal{S}}(t)$ and $\rho_{\mathcal{P}}(t)$,

$$\rho_{\mathcal{S}}(t) = \sum_s p_s|s\rangle\langle s| \quad , \quad \rho_{\mathcal{P}}(t) = \sum_s p_s\, \rho^{(s)}_{\mathcal{P}}(t)\ . \tag{24}$$

The object $\mathcal{S}$ is in one of the eigenstates $|s\rangle$ with probability p_s, in agreement with von Neumann's postulate. The pointer $\mathcal{P}$ is in the quasi-classical state $\rho_{\mathcal{P}}^{(s)}(t)$, with the same probability.

6. Quantum measurements: how long does it take?

Let us sum up the discussion of the two previous Sections about the object-pointer entanglement produced by the interaction $H_{\mathcal{PS}}$ and the decoherence arising from the coupling with the bath $H_{\mathcal{PB}}$. The dynamics implemented by $H_{\mathcal{PS}}$ uniquely ties up after the entanglement time $t_{\rm ent}$ each eigenvalue s of S with a characteristic pointer position $x_s(t)$. Neighbouring such pointer positions differ by more than the uncertainty Δ then. In absence of any other interaction, after a time $t_{\rm class} \gg t_{\rm ent}$ the initial product state has evolved into an object-pointer Schrödinger cat state. Nothing irreversible is brought about by the dynamics: the entanglement can be as easily undone as done, by applying the Hamiltonian $H_{\mathcal{PS}}$ with the parameter reset $\epsilon \to -\epsilon$. The dynamics implemented by $H_{\mathcal{PB}}$ accounts for decoherence. After the decoherence time $t_{\rm dec}$, any pair of object-pointer states corresponding to macroscopically distinguishable pointer positions are entangled with almost orthogonal states of the bath. After averaging the object-apparatus state over the bath variables, one obtains an object-pointer state $\rho_{\mathcal{PS}}(t)$ in which all information about the coherences between such macroscopically distinguishable states is missing. Because of the loss of information inherent in this averaging, the dynamics is irreversible. For $t \gg t_{\rm dec}$, $\rho_{\mathcal{PS}}(t)$ has shed all coherences for pairs (s, s') of distinct eigenvalues.

An object-pointer state $\rho_{\mathcal{PS}}(t)$ describes an accomplished measurement under two conditions:

(i) all coherences $\langle s, x|\rho_{\mathcal{PS}}(t)|s', x'\rangle$ corresponding to $s \neq s'$ have disappeared, so that $\mathcal{S} + \mathcal{P}$ is in a statistical mixture of separable states like in (22); this occurs at time $t \gg t_{\rm dec}$;

(ii) the separation between the peaks of the distinguished pointer states $\rho_{\mathcal{P}}^{(s)}(t)$ reaches a macroscopic value $\Delta_{\rm class}$; this occurs at time $t_0 \gtrsim t_{\rm class}$, see (20).

Only for $t_0 \gtrsim t_{\rm class}$ can a classical observer infer a measured value s by looking at the position of the pointer. Such a "reading" of the pointer, while still a physical process in principle perturbing $\mathcal{P}$, surely cannot blur the distinction of the peaks. Rather, the pointer will behave classically under a reading, i.e., it will not noticeably react. It is clear on (20) that (ii) can hardly arise unless the object-pointer coupling constant ϵ is very large (otherwise $t_{\rm class}$ would be larger than the time duration of the measurement). This is related to the well-known amplification problem in quantum measurements [13]. One may, however, consider a different situation than that described in Section 4, in which the interaction $H_{\mathcal{PS}}$ is switched off at some time $t_{\rm int} < t_{\rm class}$. The pointer potential $V(x)$ must then be non-confining, with two potential barriers separated by a distance W as in Fig.1. If $t_{\rm int}$ is larger than $W/(\epsilon\delta s)$, the pointer dynamics allows for a subsequent amplification of the inter-peak distance. Assuming also that $\Delta \ll W \ll \epsilon\,\delta s\,T_{\mathcal{P}}$, one has $t_{\rm int} \approx W/(\epsilon\delta s) \ll T_{\mathcal{P}}$. In this situation, the small quantum system $\mathcal{S}$ must be able to perturb the pointer strongly enough in order to produce in it a "mesoscopic change" (i.e., a distance W between the peaks in its density), instead of a macroscopic change as required in Section 4. In particular, if $\rho_{\mathcal{P}}$ is a Gibbs state with position uncertainty $\Delta_{\rm th} = (k_B T/V''(0))^{1/2}$, this arises when the height $V_0 \approx W^2 V''(0)$ of the two potential barriers satisfies $k_B T \ll V_0 \ll M(\epsilon\,\delta s)^2$ (recall that ${T_{\mathcal{P}}}^2 = M/V''(0)$). Then condition (ii) will be fulfilled at time $t_0 \approx T_{\mathcal{P}}$. If moreover $V_0 \ll V''(0)(\epsilon\,\delta s\,T_{\mathcal{S}})^2$, $t_{\rm int} \ll T_{\mathcal{S}}, T_{\mathcal{P}}$ and the simplification of the Hamiltonian (2) discussed in Subsection 3.2 is valid up to time $t_{\rm int}$.

7. Partial-equilibrium apparatus initial state

As was stressed above, we are interested in a quantitative description of a quantum measurement when, unlike in the situation described in Sections 4 and 5, $\mathcal{S}$ and $\mathcal{P}$ evolve under the *simultaneous action* of $H_{\mathcal{PS}}$ and $H_{\mathcal{PB}}$. Furthermore, we will no longer assume that the decoherence time is small compared with the bath time $t_{\mathcal{B}}$; as we shall see, the bath Hamiltonian $H_{\mathcal{B}}$ then plays an important role as well. We study in this Section the object-pointer dynamics for an apparatus initially in the partial-equilibrium initial state (3).

7.1. Derivation of the result

Our starting point is the time-dependent Redfield equation (also known as the time-convolutionless master equation) [14, 15] for the object-pointer density matrix. It reads

$$\begin{aligned}\frac{\mathrm{d}\rho_{\mathcal{PS}}}{\mathrm{d}t} &= -\frac{\mathrm{i}}{\hbar}\Big[H_{\mathcal{PS}},\rho_{\mathcal{PS}}(t)\Big]+\frac{1}{\hbar^2}\int_0^t \mathrm{d}\tau\,\Big\{h(\tau)\Big[\mathrm{e}^{-\mathrm{i}\tau H_{\mathcal{PS}}/\hbar}X^\alpha\,\mathrm{e}^{\mathrm{i}\tau H_{\mathcal{PS}}/\hbar}\rho_{\mathcal{PS}}(t)\,,\,X^\alpha\Big]\\ &\quad +h(\tau)^*\Big[X^\alpha\,,\,\rho_{\mathcal{PS}}(t)\,\mathrm{e}^{-\mathrm{i}\tau H_{\mathcal{PS}}/\hbar}X^\alpha\,\mathrm{e}^{\mathrm{i}\tau H_{\mathcal{PS}}/\hbar}\Big]\Big\} \qquad (25)\end{aligned}$$

where $h(\tau)$ is the bath correlation function (10). In (25) we have neglected $H_{\mathcal{S}}$ and $H_{\mathcal{P}}$. As we have seen in Subsection 3.2, this is justified at times $t \ll T_{\mathcal{P}}, T_{\mathcal{S}}$ provided that $\rho_{\mathcal{S}}^{(0)}(t)$ is substituted to the object initial state $\rho_{\mathcal{S}}$ at the end of the calculation. As a matter of fact, the Redfield equation is valid in a perturbative regime with respect to the pointer-bath interaction. However, the result to be obtained below can be derived differently [1] by using a non-perturbative approach which only relies on the assumption $t \ll T_{\mathcal{S}}, T_{\mathcal{P}}$ and on a property of the bath coupling agent (namely, B is a sum of operators B_ν acting on single degrees of freedom of the bath). In virtue of (1) and of the formula $\mathrm{e}^{-\mathrm{i}\epsilon\tau SP/\hbar}X\mathrm{e}^{\mathrm{i}\epsilon\tau SP/\hbar} = X - \epsilon\,\tau S$, (25) yields

$$\frac{\mathrm{d}\rho_{\mathcal{PS}}}{\mathrm{d}t} = -\frac{\mathrm{i}\,\epsilon}{\hbar}[SP,\rho_{\mathcal{PS}}(t)]+\frac{1}{\hbar^2}\int_0^t \mathrm{d}\tau\,\Big\{h(\tau)[(X-\epsilon\,\tau S)^\alpha\,\rho_{\mathcal{PS}}(t)\,,\,X^\alpha]+\mathrm{h.c.}\Big\}\,. \qquad (26)$$

Hence the matrix elements of $\rho_{\mathcal{PS}}$ in the eigenbasis of S and X satisfy at time $t \ll T_{\mathcal{P}}, T_{\mathcal{S}}$

$$\begin{aligned}\frac{\partial}{\partial t}\langle s,x|\rho_{\mathcal{PS}}(t)|s',x'\rangle &= \Big[-\epsilon\Big(s\frac{\partial}{\partial x}+s'\frac{\partial}{\partial x'}\Big)+(x'^\alpha-x^\alpha)\int_0^t \mathrm{d}\tau\,\Big\{h(\tau)(x-\epsilon\,\tau s)^\alpha\\ &\quad -h(\tau)^*(x'-\epsilon\,\tau s')^\alpha\Big\}\Big]\langle s,x|\rho_{\mathcal{PS}}(t)|s',x'\rangle\,. \qquad (27)\end{aligned}$$

The solution of (27) with the initial condition $\langle s,x|\rho_{\mathcal{PS}}(0)|s',x'\rangle = \langle s|\rho_{\mathcal{S}}^{(0)}|s'\rangle\langle x|\rho_{\mathcal{P}}|x'\rangle$ reads

$$\langle s,x|\rho_{\mathcal{PS}}(t)|s',x'\rangle = \langle s|\rho_{\mathcal{S}}^{(0)}|s'\rangle\, f\left(x_s(t),x'_{s'}(t),t\right) \qquad (28)$$

wherein $x_s(t)$ and $x'_{s'}(t)$ are given by (18) and the function $f(x,x',t)$ satisfies

$$\frac{\partial f(x,x',t)}{\partial t} = \Big(x'_{s'}(-t)^\alpha - x_s(-t)^\alpha\Big)\int_0^t \mathrm{d}\tau\,\Big\{h(\tau)x_s(\tau-t)^\alpha - h(\tau)^*x'_{s'}(\tau-t)^\alpha\Big\}f(x,x',t) \qquad (29)$$

with $f(x,x',0) = \langle x|\rho_{\mathcal{P}}|x'\rangle$. The solution of (29) is

$$\begin{aligned}f(x,x',t) &= \langle x|\rho_{\mathcal{P}}|x'\rangle\exp\Big\{-\int_0^t \mathrm{d}\tau_1\int_0^{\tau_1}\mathrm{d}\tau_2\,\Big((x'_{s'}(-\tau_1)^\alpha - x_s(-\tau_1)^\alpha\Big)\Big(h(\tau_1-\tau_2)^*x'_{s'}(-\tau_2)^\alpha\\ &\quad -h(\tau_1-\tau_2)x_s(-\tau_2)^\alpha\Big)\Big\}\,. \qquad (30)\end{aligned}$$

As is well-known [16], the real and imaginary parts of the bath correlation function (10) satisfy $\Re h(-t) = \Re h(t)$ and $\Im h(-t) = -\Im h(t)$ for all times t. Substituting $\rho_{\mathcal{S}}^{(0)}$ in (28) by the time-dependent object initial state (16) and using (30), one gets

$$\langle s,x|\rho_{\mathcal{PS}}(t)|s',x'\rangle = \langle s|\rho_{\mathcal{S}}^{(0)}(t)|s'\rangle\;\langle x_s(t)|\rho_{\mathcal{P}}|x'_{s'}(t)\rangle\;\exp\left\{-D_t(x_s(t),x'_{s'}(t);s,s')-\mathrm{i}\phi_t\right\} \qquad (31)$$

where ϕ_t is a certain real phase (depending on t, x, x', s and s') which we do not specify here since it is irrelevant for decoherence, and

$$D_t(x,x';s,s') = \frac{1}{2\hbar^2}\int_0^t \mathrm{d}\tau_1 \int_0^t \mathrm{d}\tau_2 \left(x'_{s'}(-\tau_1)^\alpha - x_s(-\tau_1)^\alpha\right)\left(x'_{s'}(-\tau_2)^\alpha - x_s(-\tau_2)^\alpha\right) h(\tau_1-\tau_2)\,. \tag{32}$$

Note that (31) is valid for times $t \ll T_{\mathcal{S}}, T_{\mathcal{P}}$ only. Due to both the initial statistical independence and our special choice of the interactions, the density matrix of $\mathcal{S}+\mathcal{P}$ retains at such times a remarkably simple product structure. The first factor in (31) accounts for free evolution of the object initial state $\rho_{\mathcal{S}}$, as generated by $H_{\mathcal{S}}$, see (16). It is equal to $p_s = \langle s|\rho_{\mathcal{S}}|s\rangle$ if $s = s'$ and $t \ll T_{\mathcal{S}}$ (Subsection 3.2). The second factor is nothing but the matrix elements of the pointer operators (18). Here, the Hamiltonian $H_{\mathcal{P}}$ does not show up because of our assumption $t \ll T_{\mathcal{P}}$ and our choice of a quasi-classical initial state $\rho_{\mathcal{P}}$. Most important is now the third factor in (31); it accounts for decoherence, i.e., for the suppression of coherences with respect to pointer displacements associated with different eigenvalues $s \neq s'$. We proceed to the discussion of that "decoherence factor".

The exponent D_t appearing in (32) has the following properties:

(a) $D_t(x,x';s,s') \geq 0$ for all values of x, x', s and s';

(b) $D_t(x,x';s,s') = 0$ initially (for $t=0$) for all matrix elements and at all later times for the diagonal matrix elements ($x = x'$ and $s = s'$);

(c) $D_t(x_s(t), x'_{s'}(t); s, s') = D_{-t}(x,x';s,s')$.

The non-negativity (a) is a consequence of the fact that the correlation function $h(t)$ and its real part $\Re h(t)$ are of positive type, i.e., they have nonnegative Fourier transforms $\widehat{h}(\omega)$ and $\widehat{(\Re h)}(\omega)$. Actually, one may rewrite (32) as

$$D_t(x,x';s,s') = \frac{1}{2\hbar^2}\int_0^\infty \frac{\mathrm{d}\omega}{\pi}\widehat{(\Re h)}(\omega)\left|\int_0^t \mathrm{d}\tau (x'_{s'}(-\tau)^\alpha - x_s(-\tau)^\alpha)\mathrm{e}^{-\mathrm{i}\,\omega\tau}\right|^2 \;\geq\; 0 \tag{33}$$

where we have used $\widehat{(\Re h)}(\omega) = \widehat{(\Re h)}(-\omega)$. Property (c) is easily checked by a change of the time integration variable in (33). Let us recall from Section 4 that the dynamics generated by $H_{\mathcal{PS}}$ maps the object-pointer coordinate (x,s) into $(x_s(t),s)$ after time t and, similarly, (x',s') is mapped into $(x'_{s'}(t),s')$. Hence one may interpret (c) as the invariance of D_t under time reversal, i.e., under $t \to -t$ and the exchange of the initial and final coordinates.

7.2. Decoherence time

As it was stressed in Section 4, the object-pointer matrix elements (31) for $x_s(t) = x'_{s'}(t) = 0$,

$$\rho^{\mathrm{peak}}_{\mathcal{PS}}(t;s,s') = \langle s, x = \epsilon t s|\rho_{\mathcal{PS}}(t)|s', x' = \epsilon t s'\rangle = \langle s|\rho^{(0)}_{\mathcal{S}}(t)|s'\rangle\,\langle 0|\rho_{\mathcal{P}}|0\rangle\,\mathrm{e}^{-D_t^{\mathrm{peak}}(s,s')-\mathrm{i}\phi_t^{\mathrm{peak}}}\,, \tag{34}$$

are of particular importance for decoherence in a quantum measurement. The main difference between (34) and (21) lies in the presence of the damping factor $\exp\{-D_t^{\mathrm{peak}}(s,s')\}$ given by

$$D_t^{\mathrm{peak}}(s,s') = D_t(0,0;s,s') = \frac{\epsilon^{2\alpha}}{2\hbar^2}(s'^\alpha - s^\alpha)^2\int_0^t \mathrm{d}\tau_1\int_0^t \mathrm{d}\tau_2\,\tau_1^\alpha\tau_2^\alpha h(\tau_1-\tau_2)\,. \tag{35}$$

Note that if $\alpha = 2, 4, \ldots$ is even then $D_t^{\mathrm{peak}}(s,-s) = 0$. This means that, if moreover the spectrum of S is symmetric with respect to $s=0$, the coherences (34) for $s' = -s$ are not damped. This comes from the symmetry $x \leftrightarrow -x$ of the coupling Hamiltonian $H_{\mathcal{PB}}$ in (1), which allows for the existence of decoherence-free subspaces [17]. Due to these long-living coherences, $\mathcal{P}+\mathcal{S}$ fails to reach (at least

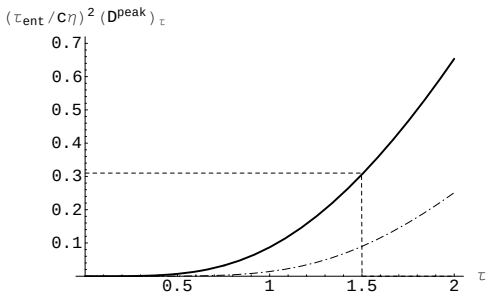

Figure 3. Decoherence exponent $D_\tau^{\rm peak}$ (multiplied by ${t_{\rm ent}}^2(\hbar\beta\eta)^{-2}$) as function of the dimensionless time $\tau = t/(\hbar\beta)$ for the harmonic oscillator bath discussed in Subsection 7.5, with $\alpha = 1$, $m = 3$ and $w_D = 2$. The intersection of the curve with the horizontal dashed line at distance ${t_{\rm ent}}^2(\hbar\beta\eta)^{-2}$ from the τ-axis gives the dimensionless decoherence time $\tau_{\rm dec}$. The dashed-dotted line is the minimal decoherence exponent $\min_{x,x'} D_\tau(x,x')$ (also multiplied by ${t_{\rm ent}}^2(\hbar\beta\eta)^{-2}$).

within a time span $t \ll T_{\mathcal{P}}, T_{\mathcal{S}}$) the statistical mixture required to be able to give a classical result to the measurement. We therefore exclude such a situation in the discussion below. In more precise words, we assume that $|s'^\alpha - s^\alpha|/|s'-s|^\alpha$ is bounded below by a constant $c_\alpha > 0$ of the order of unity, for all pairs (s,s') of eigenvalues in the spectrum of S such that $\langle s|\rho_{\mathcal{S}}|s'\rangle \neq 0$.

It is shown in Appendix A that for $s^\alpha \neq s'^\alpha$, $D_t^{\rm peak}(s,s')$ is an increasing convex function of time. This means that, quite generally, the graph of $D_t^{\rm peak}$ looks qualitatively like in Fig.3. We denote by $t_{\rm dec}(s,s')$ the time after which the coherences (34) for $s \neq s'$ are significantly damped. More precisely, this time is given by solving the implicit equation $D_{t=t_{\rm dec}}^{\rm peak}(s,s') = 1$, i.e.,

$$\left(\frac{t_{\rm ent}(s,s')}{\eta^{1/\alpha}}\right)^{2\alpha} = \frac{c_\alpha(s,s')^2}{(\hbar\beta)^2}\int_0^{t_{\rm dec}(s,s')} {\rm d}\tau_1 \int_0^{\tau_1} {\rm d}\tau_2\, \tau_1^\alpha \tau_2^\alpha\, \frac{\Re h(\tau_1-\tau_2)}{\langle B^2\rangle} \tag{36}$$

where

$$t_{\rm ent}(s,s') = \frac{\Delta}{\epsilon|s'-s|} \tag{37}$$

is the entanglement time (whose physical interpretation has been illustrated in Section 4), η is the (fluctuation of the) initial pointer-bath coupling energy in units of k_BT,

$$\eta = \langle B^2\rangle^{1/2}\Delta^\alpha\beta \;\approx\; \beta(\mathrm{tr}(H_{\mathcal{PB}}^2\,\rho_{\mathcal{P}}\otimes\rho_{\mathcal{B}}^{(\rm eq)}))^{1/2}\,, \tag{38}$$

$c_\alpha(s,s') = 1$ if $\alpha = 1$ and

$$c_\alpha(s,s') = \frac{|s'^\alpha - s^\alpha|}{|s'-s|^\alpha} \quad \text{if} \quad \alpha \geq 1\,. \tag{39}$$

By inspection on (36), $t_{\rm dec}(s,s')$ depends on the object-pointer and pointer-bath coupling constants ϵ and η through the single parameter $\epsilon\,\eta^{1/\alpha}$. Recalling that (31-36) are valid with the proviso $t \ll T_{\mathcal{S}}, T_{\mathcal{P}}$, one has to check *a posteriori* that the "free" evolutions of S and X, P are slow compared to $t_{\rm dec}(s,s')$,

$$t_{\rm dec}(s,s') \ll T_{\mathcal{S}}, T_{\mathcal{P}}\,. \tag{40}$$

If moreover $t_{\rm dec}(s,s') \geq t_{\rm ent}(s,s')$ then at time $t \gg t_{\rm dec}(s,s')$ the object-pointer coherences $\langle s,x|\rho_{\mathcal{PS}}(t)|s',x'\rangle$ are vanishingly small for all values of (x,x') . This comes from the single-peak character of the pointer initial state: As already pointed out in Section 5, for values of (x,x') such that $|x_s(t)| \gtrsim \Delta$ or $|x'_{s'}(t)| \gtrsim \Delta$ the pointer coherences $\langle x_s(t)|\rho_{\mathcal{P}}|x'_{s'}(t)\rangle$ are small. On the other hand, if (x,x') is close to $(t\epsilon s, t\epsilon s')$ with uncertainty Δ and $t \gg t_{\rm dec}(s,s') \geq t_{\rm ent}(s,s')$, i.e., if $|x_s(t)|, |x'_{s'}(t)| \lesssim \Delta \ll \epsilon t|s'-s|$, it follows from (32) and (35) that the decoherence factor $\exp\{-D_t\}$

in (31) is close to $\exp\{-D_t^{\rm peak}\}$ and is thus small. As a result, for $t \gg t_{\rm dec}(s,s')$ the product of the pointer coherence and the decoherence factor in (31) is small for all (x,x'). It is worth to emphasise that if, unlike in the situation just described, $t_{\rm dec}(s,s')$ is smaller than $t_{\rm ent}(s,s')$ then some matrix elements $\langle s,x|\rho_{\mathcal{PS}}(t)|s',x'\rangle$ may still be large at time $t_{\rm dec}(s,s')$ for some (x,x') located within a distance Δ from the centre $(\epsilon t s, \epsilon t s')$ of the peak of the pointer coherence. In such a case the decoherence time must be defined as the time t at which the minimum of $D_t(x,x';s,s')$ over all values of (x,x') is equal to 1. For $\alpha = 1$ this minimum turns out to be given by the right-hand side of (35) excepted that the range $[0,t]$ of both time integrals must be replaced by the symmetric range $[-t/2,t/2]$. It can be observed in Fig.3 that $\min_{x,x'} D_t(x,x';s,s')$ can be significantly smaller than $D_t^{\rm peak}$ at times $t \lesssim T_{\mathcal{B}}$, but it is possible to show that for $t \gg T_{\mathcal{B}}$ these two quantities differ by a numerical factor only. We refer the reader to [1] for more details.

If S has a discrete spectrum satisfying the requirements of Section 4, the decoherence time $t_{\rm dec}$ of the measurement is the largest of the times $t_{\rm dec}(s,s')$ for all pairs of distinct eigenvalues (s,s') such that $\langle s|\rho_{\mathcal{S}}|s'\rangle \neq 0$ (with the proviso $t_{\rm dec} \geq t_{\rm ent} = \Delta/(\epsilon\,\delta s)$, in the light of the discussion of the preceding paragraph). This amounts to replace $|s'^{\alpha} - s^{\alpha}|$ in (35) by its minimum value over all such pairs (s,s') (recall that $D_t^{\rm peak}$ is an increasing function of time). For $\alpha = 1$ this minimum value is by definition equal to δs (see Section 4); for $\alpha \geq 2$ it depends on the spectrum of S in a more subtle way. At times $t \gg t_{\rm dec}$, the object-pointer state (31) is very close to the separable state (22). In other words, $\mathcal{S}$ and $\mathcal{P}$ are in the statistical mixture (24) with the probabilities $p_s = \langle s|\rho_{\mathcal{S}}|s\rangle$ and with the pointer states $\rho_{\mathcal{P}}^{(s)}(t)$ given by

$$\langle x|\rho_{\mathcal{P}}^{(s)}(t)|x'\rangle = \langle x - t\epsilon s|\rho_{\mathcal{P}}|x' - t\epsilon s\rangle \, \exp\left\{-D_{-t}(x,x';s,s) - {\rm i}\phi_t\right\} \, . \tag{41}$$

The initial superpositions of eigenstates $|s\rangle$ have disappeared by indirect decoherence *via the pointer*. The pointer is in a statistical mixture of quasi-classical states having densities localised around $x = t\epsilon s$ with uncertainty Δ. The essence of quantum measurements lies in this loss of coherences: for indeed, as pointed out in Section 6 it is only when all object-pointer coherences for $s \neq s'$ are vanishingly small that a classical probability can be given for the result of the measurement. The measurement is accomplished under the supplementary condition that the distance between the nearest peaks of the pointer states (41) is macroscopic. This occurs at the time $t_{\rm class}$ given by (20). Because all our calculations are valid with the proviso $t \ll T_{\mathcal{S}}, T_{\mathcal{P}}$, one must assume for consistency that $t_{\rm class} \ll T_{\mathcal{S}}, T_{\mathcal{P}}$, in addition to (40). A situation under which this condition on $t_{\rm class}$ is not necessary has been discussed in Section 6.

It is worthwhile mentioning here that if $t_{\rm class} \gg t_{\rm dec}$, the object and pointer are never in a Schrödinger cat state as in (17). This is because in the limit in question, decoherence subdues linear superpositions faster (see the third factor in (31)) than entanglement between $\mathcal{P}$ and $\mathcal{S}$ can produce them (second factor in (31)). Due to the simultaneous action of $H_{\mathcal{PS}}$ and $H_{\mathcal{PB}}$, the whole measurement process directly produces the mixture of macroscopically distinct pointer states $\rho^{(s)}(t)$, i.e. without allowing for the intermediate appearance of superpositions of macroscopically distinguishable pointer states.

Our results (31-36) go beyond the so-called Markovian limit which would require $T_{\mathcal{B}} \ll t_{\rm dec}$. This is an important point, since for sufficiently large ϵ decoherence takes place within the "non-Markovian" regime $t \lesssim T_{\mathcal{B}}$. Explicit asymptotical results for $t_{\rm dec}$ can now be drawn from the foregoing expressions, both for $t_{\rm dec} \ll t_{\mathcal{B}}$ and $t_{\rm dec} \gg T_{\mathcal{B}}$.

7.3. The short-time regime $t_{\rm dec} \ll t_{\mathcal{B}}$

In this (non-Markovian) regime, the dynamics is dominated by the interactions $H_{\mathcal{PS}}$ and $H_{\mathcal{PB}}$. For $t \ll t_{\mathcal{B}}$, one may approximate $h(\tau)$ in (35) by the thermal variance $h(0) = \langle B^2\rangle = {\rm tr}_{\mathcal{B}}(B^2\rho_{\mathcal{B}}^{(\rm eq)})$ of the bath coupling agent. In view of (37-39) this yields

$$D_t^{\rm peak}(s,s') = \left(\frac{t}{t_{\rm dec}(s,s')}\right)^{2\alpha+2} \quad , \quad t_{\rm dec}(s,s') = \left(\frac{\sqrt{2}(\alpha+1)}{c_\alpha(s,s')}\right)^{\frac{1}{\alpha+1}} \left(\frac{t_{\rm ent}(s,s')}{\hbar\beta\,\eta^{1/\alpha}}\right)^{\frac{\alpha}{\alpha+1}} \hbar\beta \, . \tag{42}$$

That result makes sense with the proviso $t_{\rm dec}(s,s') \ll t_{\mathcal{B}}, T_{\mathcal{S}}, T_{\mathcal{P}}$. The fact that $D_t^{\rm peak} \propto t^{2\alpha+2}$ could be expected from the results of Sections 4 and 5: Indeed, for fixed x and x' and $H_{\mathcal{PS}} = 0$, it has been argued that the object-pointer coherences $\langle s,x|\rho_{\mathcal{PS}}(t)|s',x'\rangle$ decay like the gaussian $\exp\{-t^2(x'^\alpha - x^\alpha)^2\langle B^2\rangle/(2\hbar^2)\}$ when $t \ll t_{\mathcal{B}}, T_{\mathcal{P}}$; recalling that for $H_{\mathcal{PS}}$ given by (1) the positions of the peaks grow proportionally with time, we recover the aforementioned power law.

It has been stressed above that the interpretation of $t_{\rm dec}$ as the decoherence time of the measurement relies on the assumption $t_{\rm ent} \leq t_{\rm dec}$. We now argue that this condition is fulfilled if the pointer-bath initial coupling energy is of the order or smaller than k_BT (i.e., $\eta \lesssim 1$) and s'/s is not very close to unity. In fact, under these assumptions one has even $t_{\rm ent}(s,s') \ll t_{\rm dec}(s,s')$. This follows from (42), the consistency condition $t_{\rm dec}(s,s') \ll t_{\mathcal{B}}$ and the inequality $t_{\mathcal{B}} \leq \hbar\beta$, which imply $t_{\rm dec}(s,s') \ll \hbar\beta$ and thus $t_{\rm ent}(s,s') \ll \hbar\beta$. In contrast, if $\alpha \geq 2$ and $|s'/s - 1| \ll 1$ one sees by inspection on (39) that $c_\alpha(s,s') \simeq \alpha|1 - s'/s|^{1-\alpha} \gg 1$. Hence the first factor in the right-hand side of the second equation in (42) is small and one may have $t_{\rm ent}(s,s') \geq t_{\rm dec}(s,s')$. A similar conclusion holds when $\eta \gg 1$.

It is worthwhile comparing the strength of decoherence for different values of the exponent α in the coupling Hamiltonian $H_{\mathcal{PB}}$, keeping its magnitude η/β in (38) constant. We find that $t_{\rm dec}$ is smaller in the nonlinear case $\alpha > 1$ in comparison with the linear case $\alpha = 1$ by a factor ${t_{\rm dec}}^{(\alpha>1)}/{t_{\rm dec}}^{(\alpha=1)}$ of the order of $({t_{\rm ent}}/{t_{\rm dec}}^{(\alpha=1)})^{(\alpha-1)/(\alpha+1)} \ll 1$. Interestingly, a linear pointer-bath coupling is less efficient than a nonlinear one in suppressing the coherences (34) for $s \neq s'$.

It should also be noted that $t_{\rm dec}$ depends on the bath through the single parameter η. This comes from the fact that the bath dynamics can be ignored when $t \ll t_{\mathcal{B}}$. Actually, (42) can be obtained directly, without relying on the general results (34) and (35), by setting $H = H_{\mathcal{PS}} + H_{\mathcal{PB}}$ in (8) and performing a calculation similar to the calculation of the decoherence time in [11].

7.4. The Markov regime $t_{\rm dec} \gg T_{\mathcal{B}}$

When $t_{\rm dec} \gg t_{\mathcal{B}}$ the off-diagonal matrix elements (34) have no time to decay between $t = 0$ and $t_{\mathcal{B}}$. Decoherence may then take place within the so-called Markov regime $t \gg T_{\mathcal{B}}$, also known in the mathematical literature as the singular-coupling limit [20]. Note that under our condition $t_{\rm dec} \ll T_{\mathcal{S}}$ it is not appropriate to use a rotating-wave approximation. The value of the decoherence time $t_{\rm dec}$ is governed in this regime by the small-frequency behaviours of the Fourier transforms of the real and imaginary parts of $h(t)$, $(\widehat{\Re h})(\omega)$ and $(\widehat{\Im h})(\omega)$. We assume that $(\widehat{\Im h})(\omega) \sim -{\rm i}\,\widehat{\gamma}\,\omega^m$ for $\omega \ll {T_{\mathcal{B}}}^{-1}$, $\widehat{\gamma}$ being a positive constant. Bearing in mind that $(\widehat{\Im h})(\omega)$ is an odd function of ω and must be regular enough (i.e., admit differentials of sufficiently high orders) in such a way that $\Im h(t)$ decays rapidly to zero as $t \to \pm\infty$, we take m to be a positive odd integer. By analogy with the case of a bath of harmonic oscillators linearly coupled to $\mathcal{P}$, we speak of *Ohmic damping* when $m = 1$ and of *super-Ohmic damping* when $m > 1$ [18, 19]. It is shown in Appendix A that in the Ohmic case $m = 1$,

$$D_t^{\rm peak}(s,s') = \left(\frac{t}{t_{\rm dec}(s,s')}\right)^{2\alpha+1} \qquad \text{(Ohmic)} \quad , \tag{43}$$

$$t_{\rm dec}(s,s') = \left(\frac{(2\alpha+1)\,\langle B^2\rangle\,\hbar\beta}{c_\alpha(s,s')^2\int_0^\infty {\rm d}\tau\,\Re h(\tau)}\right)^{\frac{1}{2\alpha+1}} \left(\frac{t_{\rm ent}(s,s')}{\hbar\beta\,\eta^{1/\alpha}}\right)^{\frac{2\alpha}{2\alpha+1}} \hbar\beta \tag{44}$$

and in the super-Ohmic case $m \geq 3$

$$D_t^{\rm peak}(s,s') = \left(\frac{t}{t_{\rm dec}(s,s')}\right)^{2\alpha} \qquad \text{(super-Ohmic)} \quad , \tag{45}$$

$$t_{\rm dec}(s,s') = \left(\frac{2\,\langle B^2\rangle\,\hbar^2\beta^2}{c_\alpha(s,s')^2|\int_0^\infty {\rm d}\tau\,\tau\,\Re h(\tau)|}\right)^{\frac{1}{2\alpha}} \frac{t_{\rm ent}(s,s')}{\eta^{1/\alpha}} \tag{46}$$

with the proviso $t_{\rm dec}(s,s') \ll T_{\mathcal{S}}, T_{\mathcal{P}}$ and $t_{\rm dec}(s,s') \gg T_{\mathcal{B}}$. We can interpret the growth of $D_t^{\rm peak}$ like $t^{2\alpha+1}$ in the Ohmic case by saying that for fixed x and x', in the Markov regime D_t must be proportional

to $t(x'^{\alpha} - x^{\alpha})^2$ (the fact that $D_t \propto t$ is well-known [3]); the indicated time behaviour of $D_t^{\rm peak}$ then follows by replacing (x, x') by $(\epsilon t s, \epsilon t s')$. Since $|h(\tau)| \leq h(0) = \langle B^2 \rangle$ and $\Re h(\tau) \simeq 0$ for $\tau \gg T_{\mathcal{B}}$ (Subsection 3.1), the integrals $\int_0^\infty {\rm d}\tau\, \Re h(\tau)$ and $|\int_0^\infty {\rm d}\tau\, \tau\, \Re h(\tau)|$ are at most of the order of $\langle B^2 \rangle T_{\mathcal{B}}$ and $\langle B^2 \rangle {T_{\mathcal{B}}}^2$, respectively. If $|s'/s - 1|$ is not close to unity (so that $c_\alpha(s, s')$ in (39) is not very large) the factor inside the parenthesis in (46) is of the order of $(\hbar\beta/T_{\mathcal{B}})^2$ or smaller. Thus, for coupling strength $\eta \lesssim \hbar\beta/T_{\mathcal{B}}$ the condition $t_{\rm ent}(s, s') \leq t_{\rm dec}(s, s')$ holds in the Markov regime for super-Ohmic baths. The situation is different for Ohmic baths: then by (44) the condition in question is violated even for small η if the entanglement time $t_{\rm ent}(s, s')$ is large enough compared with $\hbar\beta$. More precisely, still assuming that $c_\alpha(s, s')$ is of the order of unity in (44), $t_{\rm dec}(s, s')$ becomes smaller than $t_{\rm ent}(s, s')$ when

$$\frac{t_{\rm ent}(s, s')}{\hbar\beta} \gtrsim \frac{\langle B^2 \rangle \hbar\beta}{\eta^2 \int_0^\infty {\rm d}\tau\, \Re h(\tau)}\,. \tag{47}$$

For super-Ohmic baths, the decoherence time (46) decreases by increasing α for $\eta \lesssim \hbar\beta/T_{\mathcal{B}}$ and $|s'/s - 1|$ not close to unity, i.e., provided that $t_{\rm dec}(s, s') \geq t_{\rm ent}(s, s')$. Otherwise the reverse statement holds. For Ohmic baths and if $c_\alpha(s, s') \approx 1$ and $t_{\rm ent}(s, s')$ satisfies (47), we find that $t_{\rm dec}(s, s')$ is larger in the nonlinear case $\alpha > 1$ than in the linear case $\alpha = 1$ by a factor ${t_{\rm dec}}^{(\alpha>1)}/{t_{\rm dec}}^{(\alpha=1)}$ of the order of $({t_{\rm ent}}/{t_{\rm dec}}^{(\alpha=1)})^{(2\alpha-2)/(2\alpha+1)} \geq 1$. This means that nonlinear pointer-bath couplings become less efficient than a linear coupling as soon as $t_{\rm ent}(s, s')$ is large enough so as to fulfil (47). This is in striking contrast with the super-Ohmic case: then, for a fixed weak enough pointer-bath coupling strength η, nonlinear object-pointer couplings always win over a linear coupling in efficiency for decoherence.

Finally, it is worth mentioning that in the Markov regime Ohmic baths win in efficiency over super-Ohmic baths. Actually, $({t_{\rm dec}}^{\rm Ohm}/{t_{\rm dec}}^{\sup\,\rm Ohm})^{2\alpha+1}$ is equal up to a numerical factor of the order of unity to the product of $|\int_0^\infty {\rm d}\tau\, \tau\, \Re h(\tau)|(\hbar\beta \int_0^\infty {\rm d}\tau\, \Re h(\tau))^{-1}$ by $\hbar\beta/{t_{\rm dec}}^{\sup\,\rm Ohm}$. Since the last factor must be small compared with 1 for consistency (recall that $\hbar\beta \leq T_{\mathcal{B}}$), it follows that ${t_{\rm dec}}^{\rm Ohm}(s, s')$ is smaller than ${t_{\rm dec}}^{\sup\,\rm Ohm}(s, s')$.

7.5. Bath of harmonic oscillators linearly coupled to $\mathcal{P}$

To study the transition between the limiting time regimes discussed in the two preceding Subsections, let us consider a bath of $N \gg 1$ harmonic oscillators, $H_{\mathcal{B}} = \sum_\nu \hbar\omega_\nu (b_\nu^\dagger b_\nu + 1/2)$, coupled to the pointer via a coupling agent B linear in each of its creation and annihilation operators $b_\nu^\dagger$ and b_ν, $B = \sum_\nu (\kappa_\nu b_\nu^\dagger + \kappa_\nu^* b_\nu)/\sqrt{N}$ [18]. Here ω_ν is the frequency and κ_ν the coupling constant of the νth oscillator. We shall take the following specific choice for the power spectrum function:

$$J(\omega) = \frac{\pi}{N} \sum_{\nu=1}^{N} |\kappa_\nu|^2 \delta(\omega - \omega_\nu) = \widehat{\gamma}\, \omega^m {\rm e}^{-\omega^2/\omega_D^2} \tag{48}$$

wherein m is an odd positive integer, $\widehat{\gamma} > 0$ and ω_D is a cut-off frequency. The case $m = 1$ corresponds to the so-called Ohmic damping, whereas one speaks of super-Ohmic damping for $m > 1$. For instance, $m = d$ or $d + 2$ for a phonon bath in d dimensions, depending on the underlying symmetries [19]. As is well-known [18, 19] for such a harmonic oscillator bath with a linear interaction the imaginary part of the bath function (10) is temperature-independent. Moreover, its Fourier transform is given by ${\rm i}(\widehat{\Im h})(\omega) = J(\omega)$ for $\omega \geq 0$. By the KMS property (see Appendix A) this implies $(\widehat{\Re h})(\omega) = \coth(\hbar\beta\omega/2) J(|\omega|)$. If $w_D = \hbar\omega_D\beta > 1$, the thermal time $T_{\mathcal{B}} = \hbar\beta$ is the largest decay time of $\Re h(t)$. The other time scale characterising the variations of $\Re h(t)$ is the inverse Debye frequency $t_{\mathcal{B}} = \omega_D^{-1} < T_{\mathcal{B}}$. By (36), the decoherence and entanglement times in units of $T_{\mathcal{B}}$, $\tau_{\rm dec} = t_{\rm dec}/(\hbar\beta)$ and $\tau_{\rm ent} = t_{\rm ent}/(\hbar\beta)$, are given by

$$\frac{\tau_{\rm ent}^{2\alpha}}{c_\alpha^2\, \eta^2} = \frac{\int_0^\infty dw\, \coth(w/2)\, w^m\, {\rm e}^{-w^2/w_D^2} |\int_0^{\tau_{\rm dec}} {\rm d}\tau\, \tau^\alpha\, {\rm e}^{-{\rm i}w\tau}|^2}{2 \int_0^\infty dw\, \coth(w/2)\, w^m\, {\rm e}^{-w^2/w_D^2}} \tag{49}$$

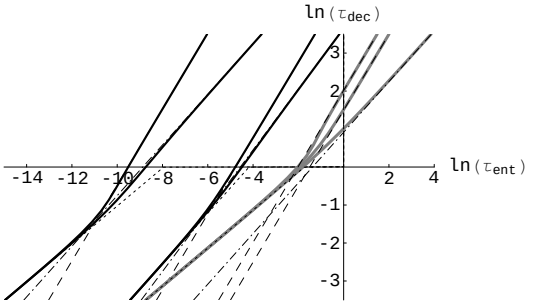

Figure 4. Decoherence vs entanglement times in units of $\hbar\beta$ in a log-log scale for the same bath as in Fig 3. The four black curves in full lines on the left correspond to $\eta = 10^{-3}$, $w_D = 10$ and $(\alpha, m) = (1,3), (1,1), (2,3)$ and $(2,1)$ (from left to right); for the three gray curves on the right $\eta = 0.5$, $w_D = 2$ and $(\alpha, m) = (1,5), (1,3)$ and $(1,1)$ (from left to right). For $\alpha = 2$ we take $c = 1$. The broken lines show the approximate expressions for $\tau_{\rm dec} \ll w_D^{-1}$ (dotted lines) and $\tau_{\rm dec} \gg 1$ (broken lines for $m = 3, 5$, dashed-dotted lines for $m = 1$), see (42), (44) and (46).

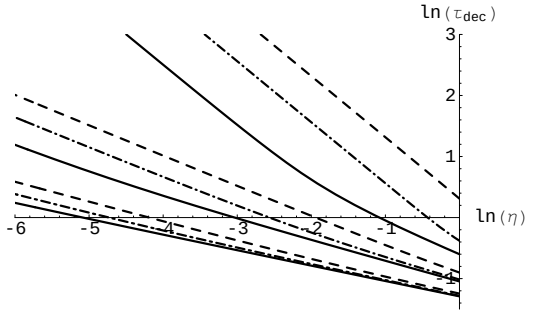

Figure 5. Decoherence time $\tau_{\rm dec}$ in units of $\hbar\beta$ as function of the pointer-bath coupling strength η in a log-log scale for the same bath as in Fig 3 with $\tau_{\rm ent} = 0.1$, $m = 3$ and $c = 1$. Three distinct values of w_D are shown: $w_D = 2$ (full lines), $w_D = 5$ (dashed-dotted lines) and $w_D = 10$ (broken lines). For each of these values, $\tau_{\rm dec}$ is shown for $\alpha = 1, 2$ and 3 (from top to bottom).

where we have expressed $\Re h(t)$ in terms of its Fourier transform (see (33)) and relied on (48). We did not write explicitly in (49) the dependence of $\tau_{\rm ent}$ and $\tau_{\rm dec}$ in (s, s'). The right-hand side of (49) is shown in Fig.3. We have computed numerically the integrals appearing in this right-hand side for various values of α, m and w_D, so as to obtain $\tau_{\rm dec}$ as function of $\tau_{\rm ent}$ and η. The main results are shown in Fig.4 and 5 in a log-log scale. For fixed α and η, the plain curves representing $\tau_{\rm dec}$ in Fig.4 split by increasing $\tau_{\rm ent}$ into distinct branches corresponding to distinct m's, as predicted by (43) and (45). This splitting occurs when $\tau_{\rm dec}$ is in the transition region $w_D^{-1} \lesssim \tau_{\rm dec} \lesssim 1$. After this splitting $\tau_{\rm dec}$ is larger for larger m so that, in particular, a Ohmic bath ($m = 1$) has a lower decoherence time than a super-Ohmic bath ($m = 3, 5 \ldots$) as stated above. For comparison, the power law behaviours found in Subsection 7.3 and 7.4 in the small time ($\tau_{\rm dec} \ll w_D^{-1}$) and Markov ($\tau_{\rm dec} \gg 1$) regimes are also shown in Fig.4 (broken lines). A remarkably good agreement between the exact and asymptotic behaviours of $\tau_{\rm dec}$ is obtained: the exact results are well approximated by their small-time behaviours (42) up to $\tau_{\rm dec} \leq w_D^{-1}$ and they are hardly distinguishable from the Markov approximation as soon as $\tau_{\rm dec} \geq 1$ (or $\tau_{\rm dec} \geq 10$ for the gray curve corresponding to $\eta = 0.5$). Our aforementioned statement that a nonlinear pointer-bath coupling is more efficient for decoherence than a linear one when $\tau_{\rm ent}$ is not too large (and even for arbitrarily large $\tau_{\rm ent}$ if $m \geq 3$ and $\eta \lesssim 1$) is well confirmed. Indeed, it is seen in Fig.4 and 5 that $\tau_{\rm dec}$ becomes significantly smaller when the value of α is increased from $\alpha = 1$ to $\alpha = 3$. If the broken lines showing $\ln(\tau_{\rm dec})$ above the horizontal axis would be drawn further to the right in Fig.4, those lines corresponding to distinct α and fixed $m = 1$ would intersect; after this intersection (not shown in the figure) the reverse situation of higher values of α leading to higher values of $\tau_{\rm dec}$ occurs. In contrast, for $m = 3, 5, \ldots$ the broken lines associated with distinct α's never intersect (their are all parallel to the line $\ln(\tau_{\rm dec}) = \ln(\tau_{\rm ent})$); hence $\tau_{\rm dec}$ decreases with α and $\tau_{\rm ent} \leq \tau_{\rm dec}$ for all values of $\tau_{\rm ent}$. We also emphasise that $\tau_{\rm dec}$ increases in Fig. 5 with the Debye cut-off frequency ω_D. Even though the results in Fig.4 and 5 correspond to the simplifying choice of a bath of harmonic oscillators with power spectrum function (48), for more general baths these figures should give the correct qualitative picture.

8. Equilibrium apparatus initial state

We now turn to the initial state (4), i.e., to a pointer and bath initially entangled and locally in thermal equilibrium. Our result for this initial state looks quite similar to that for the initial state (3) discussed in Section 7. We shall here only state this result, postponing the details of its proof to [1]. Let us first introduce the pointer effective potential

$$V_{\rm eff}(x) = V(x) - \hbar^{-1}\gamma_0\, x^{2\alpha} \;, \tag{50}$$

wherein γ_0 is given in terms of the imaginary part of the bath correlation function $h(t)$ by

$$\gamma_0 = \int_{-\infty}^{0} \mathrm{d}\tau\, \Im h(\tau) \;. \tag{51}$$

We write $Z_{\mathcal{P},\rm eff} = \int \mathrm{d}x\, \mathrm{e}^{-\beta V_{\rm eff}(x)}$ for the partition function associated with $V_{\rm eff}$. It can be shown with the help of the KMS property (A2) and the positivity of $(\widehat{\Re h})(\omega)$ that $\gamma_0 \geq 0$. Considering e.g. a linear pointer-bath coupling, $\gamma_0/\hbar$ is the mean force per unit length exerted by the bath on the pointer. Note that $V_{\rm eff}(x)$ is a non-confining potential if $V(x) = o(x^{2\alpha})$ at large distances. For instance, if $\mathcal{P}$ is a harmonic oscillator ($V(x) \propto x^2$ for all x) and $\alpha > 1$ then $V_{\rm eff}(x)$ looks like in Fig. 1. This means that an initial pointer density localised around $x = 0$ will eventually spread over the whole real line via tunnel effect after the pointer-bath coupling (1) is switched on. Our result for the initial state (4) relies, in addition to $t \ll T_{\mathcal{P}}, T_{\mathcal{S}}$, on the two following additional hypotheses: (a) the separation of time scales $\hbar\beta \ll T_{\mathcal{P}}$ or, equivalently, the separation of length scales $\lambda_{\rm th} \ll \Delta_{\rm th}$ (Section 2); (b) a weak enough pointer-bath coupling satisfying

$$\eta_{\rm th} < 1/\sqrt{2} \quad \text{if} \quad \alpha = 1 \quad , \quad \eta_{\rm th} \ll 1 \quad \text{if} \quad \alpha > 1 \tag{52}$$

where $\eta_{\rm th}$ is given by (38) with $\Delta = \Delta_{\rm th} = (\beta V''(0))^{-1/2}$. Condition (52) is motivated by the following requirement: The effective potential (50) must have a local minimum at $x = 0$ and the width and height of the potential well at the origin must be much larger than $\Delta_{\rm th}$ and $k_B T$, respectively (see Fig. 1). If this requirement is not fulfilled then, due to the instability induced by the coupling $H_{\mathcal{PB}}$, it is not possible to prepare a pointer-bath initial equilibrium-like state $\rho^{(\rm eq)}_{\mathcal{PB}}$ with a pointer density $\langle x|\,\mathrm{tr}_{\mathcal{B}}(\rho_{\mathcal{PB}})|x\rangle$ having a single peak at the origin as discussed in Section 2. We exclude here such a possibility, henceforth also excluding the occurrence of symmetry breaking and phase transitions considered in [5]. It is shown in [1] that (52) implies the required stability of $V_{\rm eff}(x)$.

We can now state our result for the object-pointer density operator when $\mathcal{P}$ and $\mathcal{B}$ are initially in the state (4). For $\alpha = 1$, it is given at times $t \ll T_{\mathcal{S}}, T_{\mathcal{P}}$ by

$$\langle s, x|\rho_{\mathcal{PS}}(t)|s', x'\rangle = \langle s|\rho^{(0)}_{\mathcal{S}}(t)|s'\rangle\, \exp\left\{-D_t(x_s(t), x_{s'}(t); s, s') - \mathrm{i}\phi'_t\right\} R_0(x_s(t), x'_{s'}(t)) \tag{53}$$

wherein D_t is the same decoherence exponent as before, see (32), ϕ'_t is a real phase and

$$R_0(x, x') = Z^{-1}_{\mathcal{P},\rm eff}\, \mathrm{e}^{-\beta(V_{\rm eff}(x)+V_{\rm eff}(x'))/2}\, \mathrm{e}^{-2\pi^2(x'-x)^2)/\lambda^2_{\rm th}} \;. \tag{54}$$

The only difference between (53) and the formula (31) for the partial-equilibrium initial state lies in the replacement of the initial pointer density $\langle x|\rho_{\mathcal{P}}|x'\rangle$ by the Gibbs-like density $R_0(x, x')$. Interestingly, (53) entails the following result on the reduced pointer initial state $\rho_{\mathcal{P}} = \mathrm{tr}_{\mathcal{B}}(\rho_{\mathcal{PB}})$

$$\langle x|\,\mathrm{tr}_{\mathcal{B}}(\rho_{\mathcal{PB}})|x'\rangle = R_0(x, x') \;. \tag{55}$$

Comparing (54) with the expression of $\langle x|\rho^{(\rm eq)}_{\mathcal{P}}|x'\rangle$ at high-temperatures given in Section 2, we see that under the aforementioned conditions (a) and (b) the coupling between $\mathcal{P}$ and $\mathcal{B}$ can be fully accounted for by the effective potential (50). Furthermore, for a linear coupling $\alpha = 1$, the matrix elements (55) can be

approximated for small x and x' by the Gaussian (7) with an almost unchanged uncertainty in momentum $\Delta p \simeq 2\pi\hbar/\lambda_{\rm th}$ and a renormalised uncertainty in position $\Delta_{\rm eff}$ given by $\Delta_{\rm eff}^{-2} = \beta(V''(0) - 2\gamma_0/\hbar)$. Note that (52) entails $\Delta_{\rm th} \leq \Delta_{\rm eff} \leq \sqrt{2}\Delta_{\rm th}$. The analog of (34) for the equilibrium-apparatus initial state is

$$\rho_{\mathcal{PS}}^{\rm peak}(t;s,s') = \langle s|\rho_{\mathcal{S}}^{(0)}(t)|s'\rangle\, R_0(0,0)\, {\rm e}^{-D_t^{\rm peak}(s,s')-{\rm i}\phi_t^{\rm peak\prime}} \tag{56}$$

where $D_t^{\rm peak}$ is given by (35). For $\alpha = 2$, one has at times $t \ll T_{\mathcal{S}}, T_{\mathcal{P}}$

$$\langle s,x|\rho_{\mathcal{PS}}(t)|s',x'\rangle = \langle s|\rho_{\mathcal{S}}^{(0)}(t)|s'\rangle\, \exp\left\{-D_t(x_s(t),x_{s'}(t);s,s')\right\} \frac{{\rm e}^{-{\rm i}\phi_t''}\, R_0(x_s(t),x'_{s'}(t))}{(1+4g_t^2(x,x';s,s'))^{1/4}} \tag{57}$$

wherein D_t and R_0 are given by (32) and (54), ϕ_t'' is a real phase and

$$g_t(x,x';s,s') = (8\pi^2)^{-\frac{\alpha}{2}}\, \frac{\lambda_{\rm th}^\alpha}{\hbar^2} \int_0^t {\rm d}\tau_1 \int_{-\infty}^{\tau_1} {\rm d}\tau_2\, \Im h(\tau_2)\left((x'_{s'}(-\tau_1)^\alpha - x_s(-\tau_1)^\alpha\right) . \tag{58}$$

It can be shown [1] that for $\alpha > 1$, (52) entails $g_t(x,x';s,s')^2 \ll (\lambda_{\rm th}/\Delta_{\rm th})^2 D_t(x,x';s,s')$. The denominator in (57) is thus close to unity if condition (a) holds and $D_t(x,x';s,s') \lesssim 1$. Therefore, in the interesting regime $0 \leq t \lesssim t_{\rm dec}(s,s')$, (56) gives a good approximation of $\rho_{\mathcal{PS}}^{\rm peak}(t;s,s')$ for $\alpha = 2$ as well. It is argued in [1] that this is still true for higher α's.

It follows from (53-57) that the coherences of $\rho_{\mathcal{PS}}(t)$ for $s \neq s'$ decay with the same rate for the initial states (3) and (4), at least in the early time regime $0 \leq t \lesssim t_{\rm dec}$. Furthermore, in view of (54) the whole discussion of Section 4 about the emergence of classically discernible peaks remains qualitatively valid. Hence our result for the equilibrium apparatus initial state goes a long way towards supporting the general conclusions about quantum measurement of Section 7. In particular, $t_{\rm dec}$ is given by (42), (44) and (46) in the short-time and Markov limits and it behaves like in Fig.4 and 5 in the intermediate region between these two limits.

9. Conclusion

Let us summarise the main results of this paper. The model for a quantum measurement presented in Section 2 has five parameters: the object-pointer coupling constant ϵ, the thermal variance $\langle B^2\rangle$ of the bath coupling agent, the temperature $T = (k_B\beta)^{-1}$ of the bath, the uncertainty Δ in the initial pointer position (equal to $\Delta_{\rm eff} \approx \Delta_{\rm th}$ for the initial state (4)) and the exponent α associated with the nonlinearity of the pointer-bath Hamiltonian (1). One may construct out of the first four parameters two relevant dimensionless constants. The first one is the entanglement time $\tau_{\rm ent} = \Delta(\epsilon\,\delta s\,\hbar\beta)^{-1}$ in units of the thermal time. It measures the efficiency of the pointer-bath interaction (a coupling is efficient if $\tau_{\rm ent}$ is small). More precisely, it is the time after which distinct positions of the pointer corresponding to distinct eigenvalues s begin to be resolved. The second constant is the coupling energy $\eta = \langle B^2\rangle^{1/2}\Delta^\alpha\beta$ in units of k_BT, which measures the strength of the pointer-bath interaction. We have found that the joint state (8) of the object and pointer is close to the statistical mixture of separable states (22) at times t large compared with the decoherence time $t_{\rm dec} = \hbar\beta\,\tau_{\rm dec}$ given by

$$\tau_{\rm dec} \propto \left(\eta^{-1/\alpha}\tau_{\rm ent}\right)^\gamma\ ,\ \gamma = \begin{cases} \frac{\alpha}{\alpha+1} & \text{if} \quad t_{\rm dec} \lesssim t_{\mathcal{B}} \quad \text{(interaction-dominated regime)} \\ \frac{2\alpha}{2\alpha+1} & \text{if} \quad t_{\rm dec} \gtrsim T_{\mathcal{B}} \quad \text{for a Ohmic bath (Markov)} \\ 1 & \text{if} \quad t_{\rm dec} \gtrsim T_{\mathcal{B}} \quad \text{for a super-Ohmic bath (Markov).} \end{cases} \tag{59}$$

This formula is valid provided that $t_{\rm dec} \ll T_{\mathcal{S}}, T_{\mathcal{P}}$. We have omitted all numerical factors, which are given explicitly in (42), (44) and (46). Two distinct regimes ought to be identified in (59): in the *interaction-dominated regime*, the decoherence time is shorter than the characteristic time $t_{\mathcal{B}}$ after which

the bath correlation function $h(t)$ in (10) differs significantly from its value $\langle B^2\rangle$ at $t=0$; in the opposite *Markov regime*, one must wait more than the bath correlation time $T_{\mathcal{B}}$, i.e., the largest decay time of $h(t)$, to obtain the required statistical mixture (22). While $t_{\rm dec}$ presents a universal behaviour in the interaction-dominated regime (it depends on the bath through the parameter η only), in the Markov regime it is determined by the small-frequency behaviour of the Fourier transform of the imaginary part of $h(t)$, $(\widehat{\Im h})(\omega) \sim -{\rm i}\,\widehat{\gamma}\,\omega^m$. Larger values of $t_{\rm dec}$ are found for larger m's. Although the dependence of $t_{\rm dec}$ on m is partly hidden in the proportionality factors in (59), a significant change of behaviour between $m=1$ (Ohmic bath) and $m>1$ (super-Ohmic bath) is manifest in this equation. In both time regimes, it turns out that the value of $t_{\rm dec}$ depends strongly on the nonlinearity exponent α. Smaller decoherence times are obtained for larger α's excepted in the Markov regime if $m>1$ and $\eta \gtrsim \hbar\beta/T_{\mathcal{B}}$ or if $m=1$ and $\eta^2\tau_{\rm ent} \gtrsim \hbar\beta/T_{\mathcal{B}}$, where the reverse statement holds. Moreover, with the same restrictions one has $\tau_{\rm dec} \geq \tau_{\rm ent}$. Let us emphasise again that for a small $\tau_{\rm ent}$, the time $t_{\rm dec}$ needed for the transformation of linear superpositions into statistical mixtures can be so small that the whole measurement is performed without producing a Schrödinger cat state as an intermediate step. It would be interesting to study concrete models for the object and pointer involving projective measurements in this "no-cat" regime, in connection with recent experiments in Solid State Physics and with parametric oscillators in Quantum Optics.

Acknowledgments
We acknowledge support from the German Sonderforschungbereich SFB/TR 12 and the French Grant ANR-05-JCJC-0107-01.

Appendix A. Large-time behaviours of the decoherence exponent (35)

Let us first show that for $s^\alpha \neq s'^\alpha$, $D_t^{\rm peak}(s,s')$ is an increasing convex function of time. Actually, let us take $x=x'=0$ in (33), differentiate both sides with respect to t, integrate the remaining time integral by parts and make the variable substitution $u=\tau/t$. This yields

$$\frac{\partial}{\partial t}D_t^{\rm peak}(s,s') = \frac{\epsilon^{2\alpha}}{\hbar^2}(s'^\alpha - s^\alpha)^2\,\alpha\,t^{2\alpha}\int_0^\infty \frac{{\rm d}\omega}{\pi}\frac{(\widehat{\Re h})(\omega)}{\omega}\int_0^1 {\rm d}u\,(1-u)^{\alpha-1}\sin(\omega t u)\;. \tag{A1}$$

Using the fact that the function $(1-u)^{\alpha-1}$ is positive and decreasing between 0 and 1, it is easy to show that the integral over u in (A1) is positive for almost all $\omega \geq 0$. Bearing in mind that $(\widehat{\Re h})(\omega) \geq 0$, this establishes that $\partial D_t^{\rm peak}/\partial t > 0$. Hence $D_t^{\rm peak}$ is an increasing function of t. By a similar argument, $\partial^2 D_t^{\rm peak}/\partial t^2 > 0$ and thus $D_t^{\rm peak}$ is convex.

We now study the behaviour of $D_t^{\rm peak}$ as $t \gg T_{\mathcal{B}}$. In the light of the discussion in Subsection 7.4, we assume $(\widehat{\Im h})(\omega) \sim -{\rm i}\,\widehat{\gamma}\,\omega^m$ as $\omega \ll {T_{\mathcal{B}}}^{-1}$ with $\widehat{\gamma}>0$. The small-frequency behaviours of $(\widehat{\Re h})(\omega)$ and $(\widehat{\Im h})(\omega)$ are related by the KMS relation $\widehat{h}(\omega) = {\rm e}^{\hbar\beta\omega}\widehat{h}(-\omega)$, i.e.

$$(\widehat{\Re h})(\omega) = \frac{{\rm i}(\widehat{\Im h})(\omega)}{\tanh(\hbar\beta\omega/2)}\;. \tag{A2}$$

Such a relation holds because the equilibrium density matrix defining $h(t)$ in (10) is a bath Gibbs state [21]. It implies $(\widehat{\Re h})(\omega) \sim 2\,\widehat{\gamma}\,\omega^{m-1}/(\hbar\beta)$. Let us first discuss the super-Ohmic case $m \geq 3$. The frequency integral in (A1) can be rewritten after an integration by parts as

$$\int_0^\infty \frac{{\rm d}\omega}{\pi}\frac{(\widehat{\Re h})(\omega)}{t\,\omega^2}\Big(1-\delta_{\alpha 1}\cos(\omega t) - (\alpha-1)\int_0^1 {\rm d}u\,(1-u)^{\alpha-2}\cos(\omega t u)\Big) \simeq \int_0^\infty \frac{{\rm d}\omega}{\pi}\frac{(\widehat{\Re h})(\omega)}{t\,\omega^2} \tag{A3}$$

where we have neglected in the right-hand side the oscillatory integrals by invoking $t \gg T_{\mathcal{B}}$. But

$$\int_0^\infty \mathrm{d}\tau\, \tau\, \Re h(\tau) = \lim_{\varepsilon\to 0+} \int_{-\infty}^{\infty} \frac{\mathrm{d}\omega}{2\pi} (\widehat{\Re h})(\omega) \int_0^\infty \mathrm{d}\tau\, \tau\, \mathrm{e}^{-\mathrm{i}(\omega-\mathrm{i}\varepsilon)\tau} = -\int_0^\infty \frac{\mathrm{d}\omega}{\pi} \frac{(\widehat{\Re h})(\omega)}{\omega^2}\,. \qquad \text{(A4)}$$

Hence, for $m \geq 3$ the frequency integral in (A1) can be approximated by $t^{-1}|\int_0^\infty \mathrm{d}\tau\, \tau\, \Re h(\tau)|$. For a Ohmic bath $m = 1$, the last integral in (A3) diverges. We now argue that one can replace $(\widehat{\Re h})(\omega)$ by $(\widehat{\Re h})(0) = 2\widehat{\gamma}(\hbar\beta)^{-1}$ in the frequency integral in (A1), which becomes

$$\int_0^\infty \frac{\mathrm{d}\omega}{\pi} \frac{(\widehat{\Re h})(0)}{\omega} \int_0^1 \mathrm{d}u\, (1-u)^{\alpha-1} \sin(\omega t u) = \frac{(\widehat{\Re h})(0)}{2\alpha} \qquad \text{(A5)}$$

in the limit $t \gg T_{\mathcal{B}}$ (we have used $\int \mathrm{d}\omega \sin(\omega t u)/\omega = \pi$ for $tu > 0$). Note that this amounts to replace $\Re h(t)$ by a white-noise correlator $(\widehat{\Re h})(0)\,\delta(t)$ in (35). Let us estimate the error introduced in the frequency integral in (A1) by this substitution. This error is given by the left-hand side of (A3) modulo the replacement of $(\widehat{\Re h})(\omega)$ by $(\widehat{\Re h})(\omega) - (\widehat{\Re h})(0)$. Disregarding oscillatory integrals as in the case $m \geq 3$, the error is equal in the limit $t \gg T_{\mathcal{B}}$ to $t^{-1}\int_0^\infty \mathrm{d}\omega\, ((\widehat{\Re h})(\omega) - (\widehat{\Re h})(0))\, \omega^{-2}/\pi$. The latter integral converges since $(\widehat{\Re h})(\omega) - (\widehat{\Re h})(0)$ behaves like ω^2 for small ω. Comparing with (A5), one concludes that the relative error introduced in (A1) by the substitution of $(\widehat{\Re h})(\omega)$ by its value for $\omega = 0$ is small, of the order of $T_{\mathcal{B}}/t$. Therefore, for $m = 1$ the frequency integral in (A1) can be approximated by $(\widehat{\Re h})(0)/(2\alpha) = \alpha^{-1}\int_0^\infty \mathrm{d}\tau\, \Re h(\tau)$. Collecting the above results and integrating (A1) with respect to t, one easily establishes (43-46).

References

[1] Spehner D and Haake F, work in progress
[2] Wheeler J A and Zurek W H 1983 *Quantum Theory and Measurement* (Princeton NJ: Princeton University Press)
[3] Giulini D, Joos E, Kiefer C, Kupsch J, Stamatescu I O and Zeh H D 1996 *Decoherence and the Appearance of a Classical Word in Quantum Theory* (Berlin: Springer)
[4] Zurek W H 1991 *Physics Today* **44** (10), 36 (updated version: *preprint* ArXiv:quant-ph/0306072)
Zurek W H 2003 *Rev. Mod. Phys.* **75**, 715-775
[5] Allahverdyan A E, Balian R and Nieuwenhuizen T M 2001 *Phys. Rev. A* **64**, 032108
Allahverdyan A E, Balian R and Nieuwenhuizen T M 2003 *Europhys. Lett.* **61**, 452
[6] Plenio M B, Knight P L 1998, *Rev. Mod. Phys.* **70**, 101
[7] Toscheck P E and Wunderlich C 2001 *Eur. Phys. J. D* **14**, 387
[8] Brune M, Hagley E, Dreyer J, Maître X, Maali A, Wunderlich C, Raimond J M and Haroche S 1996 *Phys. Rev. Lett.* **77**, 4887
[9] Ithier G, Collin E, Joyez P, Meeson P J, Vion D, Esteve D, Chiarello F, Shnirman A, Makhlin Y, Schriefl J and Schön G, *Phys. Rev. B* **72**, 134519
[10] Claudon J, Fay A, Lévy L P and Buisson O 2006 *Phys. Rev. B* **73**, 180502(R)
[11] Braun D, Haake F and Strunz W T 2001 *Phys. Rev. Lett.* **86**, 2913
Strunz W T, Haake F and Braun D 2003 *Phys. Rev. A* **67** 022101
[12] Schulman L S 1996 *Techniques and Applications of Path Integration* (New York: Wiley Classics Library)
[13] Bohm D 1951 *Quantum Theory* (Englewood Cliffs, NJ: Prentice-Hall)
[14] Redfield A G 1957 *IBM J. Res. Dev.* **1** 19
[15] Breuer H P and Petruccione F 2007 *The Theory of Open Quantum Systems* (Oxford University Press)
[16] Cohen-Tannoudji C, Dupont-Roc J and Grynberg G 1992 *Atom-photon Interactions: Basic Processes and Applications* (New York: Wiley)
[17] Lidar D A and Whaley K B 2003, in *Irreversible Quantum Dynamics*, *Lecture Notes in Physics* vol **622** ed F Benatti and R Floreanini (Berlin: Springer) p 83 (*preprint* arXiv:quant-ph/0301032)
[18] Caldeira A O and Leggett A J 1983 *Ann Phys* **149** 374-456
Caldeira A O and Leggett A J 1983 *Physica* **121A** 587-616
[19] Weiss U 1993 *Quantum Dissipative Systems* (Singapore: World Scientific)
[20] Hepp K and Lieb E H 1973 *Helv Phys Acta* **46**, 573
Gorini V and Kossakowski A 1976 *J Math Phys* **17**, 1298
[21] Bratteli O, Robinson D W 1997 *Operator Algebras and Quantum Statistical Mechanics* vol 2 (Berlin: Springer)